

Hubbard-model description of the high-energy spin-weight distribution in La_2CuO_4 J. M. P. Carmelo,^{1,2} M. A. N. Araújo,^{3,4} S. R. White,⁵ and M. J. Sampaio¹¹*Center of Physics, University of Minho, Campus Gualtar, P-4710-057 Braga, Portugal*²*Institut für Theoretische Physik III, Universität Stuttgart, D-70550 Stuttgart, Germany*³*Departamento de Física, Universidade de Évora, P-7000-671 Évora, Portugal*⁴*CFIF, Instituto Superior Técnico, Universidade Técnica de Lisboa, Avenida Rovisco Pais, 1049-001 Lisboa, Portugal*⁵*Department of Physics and Astronomy, University of California, Irvine, California 92617, USA*

(Received 27 January 2012; revised manuscript received 31 July 2012; published 20 August 2012)

The spectral-weight distribution in recent neutron scattering experiments on the parent compound La_2CuO_4 (LCO), which are limited in energy range to about 450 meV, is studied in the framework of the Hubbard model on the square lattice with effective nearest-neighbor transfer integral t and on-site repulsion U . Our study combines a number of numerical and theoretical approaches, including, in addition to standard treatments, density matrix renormalization group calculations for Hubbard cylinders and a suitable spinon approach for the spin excitations. The latter spin- $\frac{1}{2}$ spinons are the spins of the rotated electrons that singly occupy sites. These rotated electrons are mapped from the electrons by a uniquely defined unitary transformation, in which rotated-electron single and double occupancy are good quantum numbers for finite interaction values. Our results confirm that the $U/8t$ magnitude suitable to LCO corresponds to intermediate U values smaller than the bandwidth $8t$, which we estimate to be $8t \approx 2.36$ eV for $U/8t \approx 0.76$. This confirms the unsuitability of the conventional linear spin-wave theory. Our theoretical studies provide evidence for the occurrence of ground-state d -wave spinon pairing in the half-filled Hubbard model on the square lattice. This pairing applies only to the rotated-electron spin degrees of freedom, but it could play a role in a possible electron d -wave pairing formation upon hole doping. We find that the higher-energy spin spectral weight extends to about 566 meV and is located at and near the momentum $[\pi, \pi]$. The continuum weight energy-integrated intensity vanishes or is extremely small at momentum $[\pi, 0]$. This behavior of this intensity is consistent with that of the spin waves observed in recent high-energy neutron scattering experiments, which are damped at the momentum $[\pi, 0]$. We suggest that future LCO neutron scattering experiments scan the energies between 450 and 566 meV and momenta around $[\pi, \pi]$.

DOI: [10.1103/PhysRevB.86.064520](https://doi.org/10.1103/PhysRevB.86.064520)

PACS number(s): 74.72.Cj, 71.10.Fd, 71.10.Hf, 78.70.Nx

I. INTRODUCTION

The development of a better understanding of quantum magnetism is important for improving our understanding of the high-temperature cuprate superconductors. Indeed, the parent compounds of the cuprates are insulating antiferromagnets, and these less-complicated undoped systems can provide valuable information on which model Hamiltonians quantitatively describe the cuprates. Improved determination of the model Hamiltonians is essential because of the many nearby competing phases in the doped systems, easily affected by small parameters, which can now be seen because of continued improvements in numerical simulations.¹

The spectral-weight distribution in recent neutron scattering experiments on the parent compound La_2CuO_4 (LCO), which are limited in energy range to about 450 meV, raise new interesting questions.² In LCO, antiferromagnetic order occurs with a commensurate wave vector $[\pi, \pi]$, where $[\pi, \pi]$ is observed to remain commensurate for a finite level of doping. A $[\pi, \pi]$ Goldstone mode was predicted by a spin-bag model.³ A decade ago the neutron scattering experiments on LCO of Coldea *et al.*⁴ first showed sufficient details of the spin-wave spectrum to demonstrate that a simple nearest-neighbor Heisenberg model must be supplemented by a number of additional terms, including ring exchanges. These terms arise naturally out of a single-band Hubbard model with finite U/t , and several detailed studies showed that the spin-wave data in the available energy window could be successfully described by the Hubbard model using a somewhat smaller value of

$U/t \sim 6-8$ than originally thought appropriate.⁴⁻⁷ (For the effective Coulomb repulsion U in units of the bandwidth, $8t$, this refers to intermediate values, $U/8t \sim 0.75-1$.)

Part of the spin spectral weight reported in Ref. 4 was deduced to be outside the energy window. The recent improved neutron scattering experiments of Ref. 2, with a wider energy window of about 450 meV, have raised a number of questions. Surprisingly, these studies revealed that the high-energy spin waves are strongly damped near momentum $[\pi, 0]$ and merge into a momentum-dependent continuum. These results led the authors of Ref. 2 to conclude that “the ground state of La_2CuO_4 contains additional correlations not captured by the Néel-SWT [spin-wave theory] picture.”

This raises the important question of whether the more detailed results can still be described in terms of a simple Hubbard model. We show that the Hubbard model *does* describe the new neutron scattering results. Our results confirm that the U/t value suitable to LCO is in the range $U/t \in (6, 8)$. Inclusion of second- and third-neighbor hopping parameters, t' and t'' , into the Hubbard Hamiltonian lead to an interaction strength $U/t \approx 8$. Specifically, the studies of Ref. 8 have considered that the best fits to the ensemble of LCO inelastic neutron scattering points from Ref. 4 are reached for $U/t \approx 7.9$ if one includes four independent parameters, t , t' , t'' , U , and for $U/t \approx 7.1$ if one includes only t and U . Furthermore, the results of Refs. 8 and 9 reveal that as far as the LCO inelastic neutron scattering is concerned the inclusion of t' and t'' does not lead to a better quantitative fit. Accordingly, the studies

of this paper consider the half-filled Hubbard model on the square lattice with only two independent effective parameters, t and U .

Our study uses a combination of a number of numerical and theoretical approaches, including, in addition to standard treatments, density matrix renormalization group (DMRG) calculations for Hubbard cylinders^{10–12} and, since conventional linear spin-wave theory is unsuitable, a spinon operator approach for the spin excitations.^{7,13} The spinon operator approach is suitable for LCO's intermediate U/t values and corresponds to a particular case of a general operator representation that profits from the recently found model's extended global symmetry.¹⁴

An exact result valid for the Hubbard model on any bipartite lattice is that for onsite interaction $U \neq 0$ it has two global $SU(2)$ symmetries,^{15,16} which refer to a global $SO(4) = [SU(2) \otimes SU(2)]/Z_2$ symmetry.^{17,18} A recent study of the problem by one of us and collaborators reported in Ref. 14, reveals that an exact extra global c hidden $U(1)$ symmetry emerges for $U \neq 0$, in addition to the $SO(4)$ symmetry. Specifically, the Hubbard model on a bipartite lattice, such as the present square lattice, has a global $[SU(2) \otimes SU(2) \otimes U(1)]/Z_2 = [SO(4) \otimes U(1)]/Z_2 = SO(3) \otimes SO(3) \otimes U(1)$ symmetry. The index c in the designation *c hidden symmetry* is intended to distinguish it from the η -spin $U(1)$ symmetry and spin $U(1)$ symmetry in the corresponding two model's $SU(2)$ symmetries. The index c also labels the c fermions, whose occupancy configurations generate the representations of the global c hidden $U(1)$ symmetry algebra. That the latter symmetry is *hidden* follows from the fact that except in the $U/t \rightarrow \infty$ limit, its generator does not commute with the electron-rotated-electron unitary operator. As a result, for finite U/t values its expression in terms of electron creation and annihilation operators has an infinite number of terms. [The generators of the η -spin and spin $SU(2)$ symmetries commute with that unitary operator.]

The origin of the extended global symmetry is a local gauge $SU(2) \otimes SU(2) \otimes U(1)$ symmetry of the model Hamiltonian electron-interaction term first identified in Ref. 19. That local symmetry becomes for finite U and t a group of permissible unitary transformations. The corresponding local $U(1)$ canonical transformation is not the ordinary $U(1)$ gauge subgroup of electromagnetism. It is rather a "nonlinear" transformation.¹⁹

For very large U/t values the Hubbard model may be mapped onto a spin-only problem whose spins are those of the electrons that singly occupy sites. However, for intermediate U/t values this mapping generates many complicated terms in the Hamiltonian, when written in terms of electron creation and annihilation operators. Here we address that problem by expressing the Hamiltonian in terms of the rotated-electron operators, which naturally emerge from the generators of the model's symmetries.

In contrast to electrons, for rotated electrons single and double occupancy are good quantum numbers for $U/t > 0$. For large U/t values electrons and rotated electrons are the same objects. Apparently, the Hamiltonian t/U expansion is formally similar in terms of electron and rotated-electron operators. However, that is only so for very large U/t values. For instance, there are well-defined t^2/U and t^4/U^3 terms

in the Hamiltonian expression in terms of rotated-electron operators, which are identical in form for very large U/t to the corresponding terms using electron operators. However, for intermediate $U/t \in (6, 8)$, if one expresses the former t^2/U and t^4/U^3 terms in electron creation and annihilation operators, one finds many complicated higher-order t^j/U^{j-1} terms where for the half-filled case j are even integers $j = 2, 4, 6, \dots$ and $j = 4, 6, 8, \dots$, respectively. Hence, the first few terms of the Hamiltonian expression in terms of rotated-electron operators describe many higher-order electron processes. For moderate U/t the rotated-electron operators also generate a much simpler form for the energy eigenstates as well as for complicated processes involving a large number of electrons. Our spin- $\frac{1}{2}$ spinons correspond to the spin- $\frac{1}{2}$ spins of the rotated electrons that singly occupy sites, so that they are well defined for $U/t > 0$.

When one decreases U/t to the intermediate U/t values suitable for LCO, the above-mentioned Hamiltonian terms become increasingly important and generate higher-order spinon processes. Fortunately, those are simpler than the corresponding electron processes. Indeed, the use of our operational representation renders the intermediate U/t quantum problem in terms of rotated electrons similar to the corresponding large- U/t quantum problem in terms of electrons. The effect of decreasing U/t is mostly an increase of the energy bandwidth of an effective band associated with the spinon occupancy configurations. The intermediate U/t rotated-electron processes may be associated with exchange constants describing rotated-electron motion touching progressively larger numbers of sites. Within our Hubbard model's representation such Hamiltonian terms emerge naturally upon decreasing the magnitude of U/t .

Our theoretical studies provide evidence of the occurrence of ground-state d -wave spinon pairing in the half-filled Hubbard model on the square lattice. One of the few exact theorems that applies to the half-filled Hubbard model on a bipartite lattice with a finite number of sites and thus on a square lattice is that its ground state is a spin-singlet state.¹⁶ Within our spinon representation the ground-state spin-singlet N -spinon configuration corresponds to $N/2$ independent spin-neutral two-spinon configurations. Under the spin-triplet excitation one of the $N/2$ spin-singlet spinon pairs is broken. Quantitative agreement with the spin-wave spectrum obtained from our standard many-particle diagrammatic analysis is reached provided that the broken spinon pair has d -wave pairing in the initial ground state. Such a pairing refers only to the rotated-electrons spin degrees of freedom. However, it could play a role in a possible d -wave electron pairing formation upon hole doping.

Applying our approach to the new LCO high-energy neutron scattering reported in Ref. 2, we find that at momentum $[\pi, 0]$ the continuum weight energy-integrated intensity vanishes or is extremely small. Furthermore, we find that beyond 450 meV, the spectral weight is mostly located around momentum $[\pi, \pi]$ and extends to about 566 meV, suggesting directions for future experiments.

The paper is organized as follows. In Sec. II the Hubbard model on the square lattice and the basic quantities of our study are introduced. The description of the model's antiferromagnetic long-range order is addressed in Sec. III. Section IV presents a random-phase-approximation (RPA)

study of the model's coherent spin-wave spectrum and intensity. Quantitative agreement with that observed in neutron-scattering experiments is used to find the U and t values suitable to LCO. The rotated-electron description emerging from the Hubbard model on the square lattice with extended global symmetry is introduced in Sec. V. This is the only section where general electronic densities and spin densities are considered. The goal of this more general analysis is the introduction of a spinon representation suitable to the LCO intermediate values of U/t . In Sec. VI this spinon representation is used in the study of the general spin-triplet spectrum of the half-filled Hubbard model on the square lattice, which includes both the spin waves and the incoherent spin-weight continuum distribution. The comparison of the predicted spectral weights with those observed in the LCO high-energy neutron scattering is the goal of Sec. VII. Finally, Sec. VIII contains the concluding remarks.

II. THE MODEL AND THE BASIC QUANTITIES OF OUR STUDY

Most of our results refer to half filling, so that the number of lattice sites, N_a , equals the number of electrons N . The exception is the general analysis reported in Sec. V, which considers arbitrary values of the electronic density $n = N/N_a$. The Hubbard model on a square lattice with $N_a \gg 1$ sites and periodic boundary conditions reads

$$\hat{H} = t \hat{T} + U \hat{V}_D, \quad \hat{T} = - \sum_{(j,j')} \sum_{\sigma} (c_{\vec{r}_j,\sigma}^{\dagger} c_{\vec{r}_{j'},\sigma} + c_{\vec{r}_{j'},\sigma}^{\dagger} c_{\vec{r}_j,\sigma}),$$

$$\hat{V}_D = \sum_{j=1}^{N_a} (\hat{n}_{\vec{r}_j,\uparrow} - 1/2)(\hat{n}_{\vec{r}_j,\downarrow} - 1/2). \quad (1)$$

Here \hat{T} is the kinetic-energy operator in units of t , \hat{V}_D is the on-site repulsion interaction operator in units of U , $c_{\vec{r}_j,\sigma}^{\dagger}$ and $c_{\vec{r}_j,\sigma}$ are electron creation and annihilation operators with site index $j = 1, \dots, N_a$ and spin $\sigma = \uparrow, \downarrow$, and $\hat{n}_{\vec{r}_j,\sigma} = c_{\vec{r}_j,\sigma}^{\dagger} c_{\vec{r}_j,\sigma}$. The on-site repulsion interaction operator \hat{V}_D may alternatively be expressed in terms of the electron double-occupancy operator \hat{D} or single-occupancy operator \hat{Q} given by

$$\hat{D} = (\hat{N} - \hat{Q})/2; \quad \hat{Q} = \sum_{j=1}^{N_a} \sum_{\sigma=\uparrow,\downarrow} \hat{n}_{\vec{r}_j,\sigma} (1 - \hat{n}_{\vec{r}_j,-\sigma}), \quad (2)$$

respectively. The expectation values,

$$d = \frac{1}{N_a} \sum_{j=1}^{N_a} \langle GS | \hat{n}_{\vec{r}_j,\uparrow} \hat{n}_{\vec{r}_j,\downarrow} | GS \rangle,$$

$$(1 - 2d) = \frac{1}{N_a} \sum_{j=1}^{N_a} \langle GS | (\hat{n}_{\vec{r}_j,\uparrow} - \hat{n}_{\vec{r}_j,\downarrow})^2 | GS \rangle, \quad (3)$$

$$m_{AF} = \frac{1}{N_a} \sum_{j=1}^{N_a} \frac{1}{2} \langle GS | (-1)^j (\hat{n}_{\vec{r}_j,\uparrow} - \hat{n}_{\vec{r}_j,\downarrow}) | GS \rangle$$

$$\approx [1 - 2\delta S] m_{AF}^0,$$

play an important role in our study, following the strong evidence that for $U > 0$ and $N_a \rightarrow \infty$ the model's ground

state has antiferromagnetic long-range order.²⁰ In the last expression of Eq. (3) one has that j is an even integer and an odd integer for each of the two sublattices, respectively. Moreover, in that expression m_{AF}^0 stands for a mean-field sublattice magnetization that does not account for the effect of transverse fluctuations while δS does account for this effect, its value being estimated below. Specifically, m_{AF}^0 is the sublattice magnetization of the spin-density wave (SDW) state obtained in a standard mean-field treatment of the Hubbard interaction at zero absolute temperature as given, for instance, in Fig. 3 of Ref. 5.

The on-site spin operators involved in our studies read

$$\hat{s}_{\vec{r}_j,s}^x = \frac{1}{2} [\hat{s}_{\vec{r}_j,s}^+ + \hat{s}_{\vec{r}_j,s}^-]; \quad \hat{s}_{\vec{r}_j,s}^y = \frac{1}{2i} [\hat{s}_{\vec{r}_j,s}^+ - \hat{s}_{\vec{r}_j,s}^-],$$

$$\hat{s}_{\vec{r}_j,s}^+ = c_{\vec{r}_j,\downarrow}^{\dagger} c_{\vec{r}_j,\uparrow}; \quad \hat{s}_{\vec{r}_j,s}^- = c_{\vec{r}_j,\uparrow}^{\dagger} c_{\vec{r}_j,\downarrow}, \quad (4)$$

$$\hat{s}_{\vec{r}_j,s}^z = -\frac{1}{2} [\hat{n}_{\vec{r}_j,\uparrow} - \hat{n}_{\vec{r}_j,\downarrow}].$$

The index s in these operators distinguishes them from the corresponding local operators associated with the η -spin SU(2) symmetry algebra considered below in Sec. V.

Our study also involves the spin dynamical structure factors,

$$S^{\alpha\alpha'}(\vec{k}, \omega) = \frac{(g\mu_B)^2}{N_a} \sum_{j,j'=1}^{N_a} e^{-i\vec{k}(\vec{r}_j - \vec{r}_{j'})}$$

$$\times \int_{-\infty}^{\infty} dt e^{i\omega t} \langle GS | \hat{s}_{\vec{r}_j,s}^{\alpha}(t) \hat{s}_{\vec{r}_{j'},s}^{\alpha'}(0) | GS \rangle, \quad (5)$$

where $\alpha = \alpha' = x, y, z$ or $\alpha = -$ and $\alpha' = +$ and below we consider $g = 2$. It is straightforward to show that the sum rules $[1/N_a] \sum_{\vec{k}} S^{\alpha\alpha'}(\vec{k})$, where $S^{\alpha\alpha'}(\vec{k}) = [1/2\pi] \int_{-\infty}^{\infty} d\omega S^{\alpha\alpha'}(\vec{k}, \omega)$, involve the average single occupancy $(1 - 2d)$ and read

$$\frac{1}{N_a} \sum_{\vec{k}} S^{\alpha\alpha'}(\vec{k}) = \frac{(g\mu_B)^2}{4} [\delta_{\alpha,\alpha'} + 2\delta_{\alpha,-} \delta_{\alpha',+}] (1 - 2d). \quad (6)$$

In an ideal experiment all components are detected with equal sensitivity. As discussed, for instance, in Ref. 6, in that case a transfer of spectral weight from the longitudinal to the transverse part as the energy increases is observed. Hence, independent of the scattering geometry, the corresponding effective spin dynamical structure factor satisfies the sum rule,

$$\frac{1}{N_a} \sum_{\vec{k}} \frac{1}{2\pi} \int_{-\infty}^{\infty} d\omega S^{exp}(\vec{k}, \omega) = \mu_B^2 2(1 - 2d). \quad (7)$$

That the coefficient involved is $2(1 - 2d)$ rather than $3(1 - 2d)$ follows from one mode being perpendicular to the plane and thus silent in the experiment.⁶

III. THE HUBBARD MODEL ON THE SQUARE-LATTICE ANTIFERROMAGNETIC LONG-RANGE ORDER

For the range $U/t \in (0, 8)$, the antiferromagnetic long-range order may be accounted for by a variational ground state with a SDW initial trial state, such as, for instance, a

Gutzwiller projected antiferromagnetic state,²¹

$$|G\rangle = e^{-g\hat{D}}|SDW\rangle, \quad U/t < 8, \quad (8)$$

or the following related state:

$$|GB\rangle = e^{-h\hat{T}/t}e^{-g\hat{D}}|SDW\rangle, \quad U/t < 8. \quad (9)$$

Here $|SDW\rangle$ is the ground state of a simple effective mean-field Hamiltonian, such as that of Eq. (18) of Ref. 21. For $U/t \gg 1$ this order is as well accounted for by a Baeriswyl variational state,

$$|B\rangle = e^{-h\hat{T}/t}|\infty\rangle, \quad U/t \gg 1, \quad (10)$$

where $|\infty\rangle$ is the exact $U/t \rightarrow \infty$ ground state.²¹ The coefficients h and g multiplying the kinetic-energy and double-occupancy operators, respectively, in the state expressions given in Eqs. (8)–(10) are variational parameters. The above states involve as well a variational gap parameter Δ , which is expected to tend to zero as the trial state approaches the exact ground state. Indeed, that variational parameter is an infinitesimal symmetry-breaking field.

Similarly for the trial state $|SDW\rangle$, the relation

$$4[m_{AF}^0]^2 = (1 - 4d), \quad (11)$$

holds for the states $|G\rangle$, $|GB\rangle$, and $|B\rangle$. However, the corresponding function $d = d(U/t)$ is, in general, state dependent. Inversion of the simple relation provided in Eq. (11) gives

$$d = \frac{1}{4}[1 - 4[m_{AF}^0]^2]. \quad (12)$$

This is consistent with d not being affected by transverse fluctuations.

The evaluation of the ground-state energy for $|G\rangle$ and $|GB\rangle$ is for $N_a \gg 1$ an involved problem. Here we resort to an approximation, which corresponds to the simplest expression of the general form,

$$E/N = T_0 q_U + Ud; \quad T_0 = -\frac{16}{\pi^2} t, \quad (13)$$

compatible with three requirements. Those are

- (1) the relation $d = \frac{1}{4}[1 - 4[m_{AF}^0]^2]$ provided in Eq. (12) must be fulfilled;
- (2) the antiferromagnetic long-range order must occur for the whole $U/t > 0$ range;
- (3) the small- U/t expansion of the energy E/N of Eq. (13) must lack of a linear kinetic-energy term in U for $U/t \ll 1$ (except for the term Ud corresponding to the on-site repulsion).

Brinkman and Rice found $q_U = 8d(1 - 2d)$ for the original paramagnetic-state Gutzwiller approximation,²² which is lattice insensitive and thus does not account for the square-lattice antiferromagnetic long-range order. The simplest modified form of the quantity q_U suitable to a broken-symmetry ground state such that the above three conditions are met is

$$q_U = \left(\frac{U}{8t}\right) a_1^{(+)} d \left[\frac{(1 - 2d)}{4[m_{AF}^0]^2} - a_2 \right] - a_3. \quad (14)$$

Here,

$$a_1^{(\pm)} = \pi^2 \pm 4; \quad a_2 = (1 - [\pi^2/2a_1^{(+)}]), \quad (15)$$

and the coefficient a_3 is a function $a_3 = a_3(U/t)$ of U/t whose approximate limiting behaviors are

$$\begin{aligned} a_3 &= \frac{a_1^{(-)}}{8} \left[1 - \tanh\left(\frac{U}{8t} \left[\frac{4 + a_1^{(+)}}{a_1^{(-)}} \right] \right) \right], \quad U/t < 8, \\ &= -c_0[\pi/2]^2 \frac{8t}{U}, \quad U/t \gg 1, \end{aligned} \quad (16)$$

where

$$c_0 = \frac{1}{2} \left[\frac{\alpha}{4} + \frac{1}{8} \right] = 0.1462. \quad (17)$$

The corresponding estimate $\alpha = 0.6696$ is that of the Heisenberg-model studies of Ref. 20. Moreover, the quantity $4[m_{AF}^0]^2$ on the right-hand side of Eq. (14) behaves as $4[m_{AF}^0]^2 = U/8t$ for $U/t \ll 1$.

Minimization of the ground-state energy defined by Eqs. (13)–(16) with respect to d leads indeed to $d = \frac{1}{4}[1 - 4[m_{AF}^0]^2]$. The limiting behaviors of that energy are

$$\begin{aligned} E/N &\approx T_0 + Ud - \frac{1}{8\pi^2} \frac{U^2}{t}, \quad U/t \ll 1, \\ &\approx -4c_0 \frac{8t^2}{U}, \quad U/t \gg 1. \end{aligned} \quad (18)$$

We note that the small- U/t second-order coefficient reads $-[1/8\pi^2] \approx -0.0127$, in agreement with that, ≈ -0.0127 , obtained by second-order perturbation theory.²³ For $U/t \gg 1$ one recovers the known result $E/N = -4c_0[8t^2/U]$,²⁰ so that our approximation agrees with the known limiting behaviors.

The quantity $4[m_{AF}^0]^2$ on the right-hand side of Eq. (14) behaves as $4[m_{AF}^0]^2 = U/8t$ for $U/t \ll 1$. However, its U/t dependence for the range $U/t \in (0, 8)$ remains an open problem. Here we have performed DMRG calculations of $(1 - 2d)$, which, according to the relation provided in Eq. (12), is given by $(1 - 2d) = \frac{1}{2}(1 + 4[m_{AF}^0]^2)$. Hence, its U/t dependence fully determines that of $4[m_{AF}^0]^2$. The corresponding DMRG results are shown in Fig. 1. Specifically, two different-circumference cylinders were simulated as a function of U/t , with open boundary conditions in x and periodic in y , and the

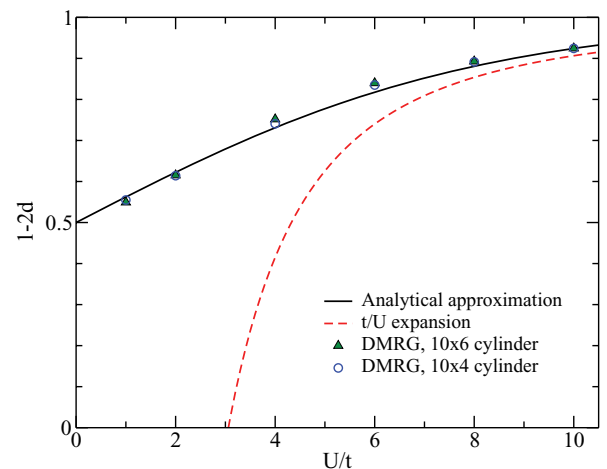


FIG. 1. (Color online) Average single-occupancy. Approximate expression $[1 + \tanh(U/8t)]/2$ valid for $U/t \leq 8$ (solid line), the limiting $U/t \gg 1$ expression $[1 - c_0(8t/U)^2]$ (dashed line), and from DMRG numerical results on two different width cylinders.

double occupancy measured in one of the middle columns. A maximum of $m = 4000$ states were kept, with an accuracy of $\sim 10^{-4}$ in $(1 - 2d)$ for the 10×4 system for the least accurate smaller U/t values and about 10^{-3} for the 10×6 system. We find that the value of $(1 - 2d)$ is relatively insensitive to cluster size, and these cluster sizes are representative of two-dimensional (2D) behavior.²⁴

We then find that $4[m_{AF}^0]^2 \approx \tanh(U/8t)$ gives for the range $U/t \in (0, 8)$ quantitative agreement for the $(1 - 2d)$ dependence on U/t with both our numerical DMRG calculations (see Fig. 1) and the numerical results for the states $|G\rangle$ and $|GB\rangle$ (see Fig. 4 of Ref. 6). For $U/t \gg 1$ we find the behavior $4[m_{AF}^0]^2 \approx e^{-2c_0(8t/U)^2}$ for the state $|B\rangle$, so that

$$(1 - 2d) \approx \frac{1}{2} \left[1 + \tanh\left(\frac{U}{8t}\right) \right], \quad U/t < 8, \\ \approx 1 - c_0 \left(\frac{8t}{U}\right)^2, \quad U/t \gg 1. \quad (19)$$

Furthermore, the states $|SDW\rangle$ and $|G\rangle$ give a sublattice magnetization $m_{AF} \approx m_{AF}^0 = \frac{1}{2}\sqrt{1 - 4d}$, with an improved U/t dependence, $d \approx \frac{1}{4}[1 - \tanh(U/8t)]$, for the latter, as follows from the corresponding $(1 - 2d)$ expression of Eq. (19). For the state $|G\rangle$ the sublattice magnetization is then given by

$$m_{AF}^0 \approx \frac{1}{2} \sqrt{\tanh\left(\frac{U}{8t}\right)}, \quad U/t < 8. \quad (20)$$

On the other hand, we find that the states $|GB\rangle$ and $|B\rangle$ have m_{AF}^{GB} and m_{AF}^B sublattice magnetization numerical values very close to those given by the relation $[1 - 2\delta S]m_{AF}^0$ of Eq. (3) with

$$\delta S \approx d, \quad U/t < 8, \\ \approx d + \frac{1}{2} \left[1 - \frac{m_{HAF}}{m_{HAF}^0} \right], \quad U/t \gg 1, \quad (21)$$

respectively. Here $m_{HAF}^0 = 1/2$ and $m_{HAF} \approx 0.303$ is the Heisenberg-model's sublattice magnetization magnitude,²⁰ so that $\delta S \approx d + 0.197$ in Eq. (21) for $U/t \gg 1$. Hence, one finds

$$m_{AF}^{GB} \approx \frac{1}{4} \left[1 + \tanh\left(\frac{U}{8t}\right) \right] \sqrt{\tanh\left(\frac{U}{8t}\right)}, \quad U/t < 8, \\ m_{AF}^B \approx \left[0.303 - 0.803 \times c_0 \left(\frac{8t}{U}\right)^2 \right], \quad U/t \gg 1. \quad (22)$$

The magnitudes of the sublattice magnetizations m_{AF}^0 and m_{AF}^{GB} as given in Eqs. (20) and (22) for the states $|G\rangle$ and $|GB\rangle$, respectively, are provided in Table I for several U/t values. In that table the magnitudes of a sublattice magnetization m_{AF}^{lower} that for $U/t > 0$ we define as $m_{AF}^{\text{lower}} =$

$(1 - 2d)[m_{HAF}/m_{HAF}^0]m_{AF}^0$ are also given. Note that for $U/t \gg 1$ the sublattice magnetization m_{AF}^{lower} becomes m_{AF}^B . Probably it is closest to the exact m_{AF} , while m_{AF}^{GB} is that consistent with our use of the RPA in the ensuing section, to study the spin-wave spectrum and corresponding intensity.

IV. COHERENT SPIN-WAVE SPECTRUM AND INTENSITY AND LCO U AND t VALUES

To study the coherent spin-wave weight distribution and spectrum, we have calculated the transverse dynamical susceptibility,

$$\chi^{-+}(\vec{k}, \tau) = \frac{(g\mu_B)^2}{N_a} \sum_{j, j'=1}^{N_a} e^{-i\vec{k}\cdot(\vec{r}_j - \vec{r}_{j'})} \langle \hat{s}_{\vec{r}_j, s}^-(\tau) \hat{s}_{\vec{r}_{j'}, s}^+(0) \rangle, \quad (23)$$

in the RPA. Here τ denotes the imaginary time in Matsubara formalism and we shall take the zero temperature limit. Because we deal with the antiferromagnetic order (Néel state) it is convenient to define two sublattices, a and b , and redefine the susceptibility as a 2×2 tensor $\tilde{\chi}_{\mu, \nu}$ where the Greek subscripts denote sublattice indices,

$$\tilde{\chi}_{\mu, \nu}^{-+}(\vec{k}, \tau) = \frac{(g\mu_B)^2}{(N_a/2)} \sum_{j \in \nu, j' \in \mu} e^{-i\vec{k}\cdot(\vec{r}_j - \vec{r}_{j'})} \langle \hat{s}_{\vec{r}_j, s}^-(\tau) \hat{s}_{\vec{r}_{j'}, s}^+(0) \rangle. \quad (24)$$

The original susceptibility in Eq. (23) is then simply related to this tensor as

$$\chi(\vec{k}, \tau) = \frac{1}{2} [\tilde{\chi}_{aa} + \tilde{\chi}_{bb} + \tilde{\chi}_{ab} + \tilde{\chi}_{ba}]. \quad (25)$$

We define electron field operators for each sublattice, $\hat{a}_{\vec{k}\sigma}$ and $\hat{b}_{\vec{k}\sigma}$, as

$$\hat{c}_{\vec{r}_j \in a, \sigma} = \frac{1}{\sqrt{N_a/2}} \sum_{\vec{k} \in RBZ} e^{i\vec{k}\cdot\vec{r}_j} \hat{a}_{\vec{k}\sigma}, \quad (26)$$

$$\hat{c}_{\vec{r}_j \in b, \sigma} = \frac{1}{\sqrt{N_a/2}} \sum_{\vec{k} \in RBZ} e^{i\vec{k}\cdot\vec{r}_j} \hat{b}_{\vec{k}\sigma}. \quad (27)$$

In the momentum summations the reduced Brillouin zone (RBZ) covers only half of the original Brillouin zone (BZ) for the square lattice. The effective Hamiltonian that describes the SDW phase in mean-field theory for the Hubbard interaction can be written as

$$\hat{H}_{\text{eff}} = \sum_{\vec{k}, \sigma} (\hat{a}_{\vec{k}\sigma}^\dagger \quad \hat{b}_{\vec{k}\sigma}^\dagger) \begin{pmatrix} \epsilon_\sigma & f(\vec{k}) \\ f(\vec{k}) & -\epsilon_\sigma \end{pmatrix} \begin{pmatrix} \hat{a}_{\vec{k}\sigma} \\ \hat{b}_{\vec{k}\sigma} \end{pmatrix}, \quad (28)$$

with

$$\epsilon_\sigma = -U \frac{\sigma}{2} m_{AF}, \quad f(\vec{k}) = -2t[\cos(k_x) + \cos(k_y)]. \quad (29)$$

TABLE I. The sublattice magnetizations as calculated here for several U/t values and some results from Refs. 6 and 21.

U/t	6.1	6.5	8.0	10.0
m_{AF}^0	0.401	0.410	0.436 [0.43 (Refs. 6 and 21)]	0.461 [0.456 (Ref. 6)]
m_{AF}^{GB}	0.329	0.342	0.384 [0.39 (Ref. 21)]	0.426
m_{AF}^{lower}	0.200	0.207	0.233	0.258

Using the effective Hamiltonian given in Eq. (28) one derives from Eq. (24) a susceptibility tensor $\tilde{\chi}_{\mu,\nu}^{(0)}(\vec{k}, \tau)$ at mean-field theory level.

Treating the Hubbard interaction further in the RPA and Fourier transforming the susceptibility from imaginary time τ to $(\vec{k}, i\omega)$ space, the susceptibility tensor then obeys the Dyson equation,

$$\tilde{\chi}^{RPA} = \tilde{\chi}^{(0)} + U \tilde{\chi}^{(0)} \tilde{\chi}^{RPA}, \quad (30)$$

which can be recast as

$$\tilde{\chi}^{RPA} = [\hat{I} - U \tilde{\chi}^{(0)}]^{-1} \tilde{\chi}^{(0)}. \quad (31)$$

Here \hat{I} stands for the 2×2 identity matrix. Such a procedure of treating the interaction in RPA on top of the mean-field solution has been used in previous studies.^{5,25}

$\tilde{\chi}^{RPA}$ has a pole $i\omega = \omega(\vec{k})$ obtained from the equation $\text{Det}[1 - U \tilde{\chi}^{(0)}] = 0$, which provides the dispersion relation $\omega(\vec{k})$ for the spin waves. It has been shown in Ref. 5 that an excellent agreement with the spin-wave spectrum from Ref. 4 is achieved. In Fig. 2 (top) we show a fit to the more recent experimental data of Ref. 2 (solid line) along with the results from the $s1$ fermion method reported below in Sec. VI (dashed line) for $U/t = 6.1$ and $t = 295$ meV. This corresponds to a bandwidth $8t \approx 2.36$ eV.

Importantly, provided that the t magnitude is slightly increased for increasing values of U/t , agreement with the LCO spin-weight spectrum and distribution can be obtained

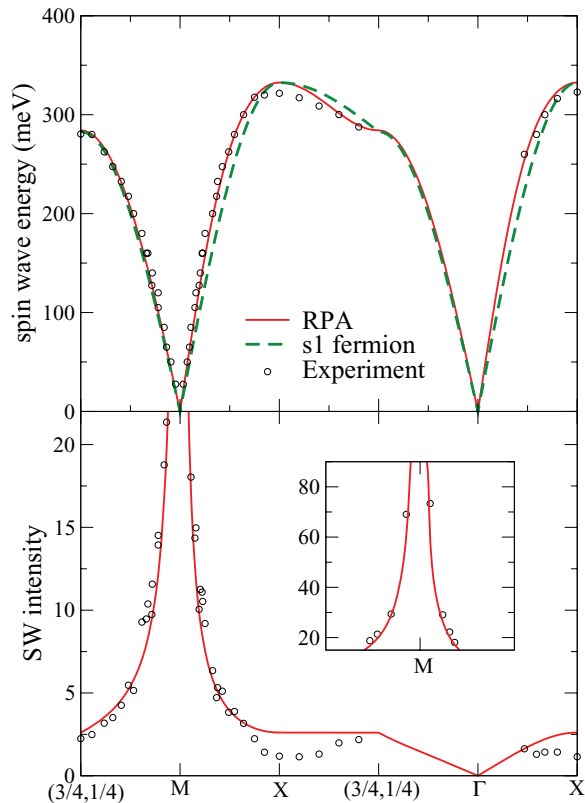


FIG. 2. (Color online) (Top) Spin-wave excitation spectrum along BZ special directions as specified in Ref. 2. (Bottom) Spin-wave intensity as obtained from the poles of the susceptibility (see text). Experimental points from Ref. 2.

for the range $U/t \in (6, 8)$ and thus $U/8t \in (0.75, 1)$ in units of the bandwidth $8t$. For U/t values smaller than 6 (and larger than 8), the spin-wave dispersion between $[\pi, 0]$ and $[\pi/2, \pi/2]$ has a too-large energy bandwidth (and is too flat) for any reasonable value of t .

Let $|v, \omega(\vec{k})\rangle$ denote the excited energy eigenstates of energy $\omega(\vec{k})$ and momentum \vec{k} that contribute to the coherent spin-wave spectral weight. In the case of the $-+$ spin dynamical structure factor given in Eq. (5) for $\alpha = -$ and $\alpha' = +$, the corresponding coherent spin-wave spectral weight in units of μ_B^2 is given by $Z_d 2(1 - 2d)$. The factor Z_d in this expression reads

$$Z_d = 1 - \frac{2}{N_a(1 - 2d)} \sum_{\vec{k}} \sum_{v' \neq v} |\langle v' | \hat{s}_{\vec{k},s}^+ | GS \rangle|^2, \quad (32)$$

where $\hat{s}_{\vec{k},s}^+$ is the Fourier transform of the spin operator $\hat{s}_{r,s}^+$ defined in Eq. (4) and the sum over energy eigenstates excludes those that generate the coherent spin-wave weight, $|v\rangle = |v, \omega(\vec{k})\rangle$. In the $U/t \rightarrow \infty$ limit, Z_d may be identified with the corresponding $Z_d = Z_c Z_\chi$ factor of the Heisenberg model on the square lattice. According to the results of Ref. 26, the factors Z_c and Z_χ have magnitudes $Z_c \approx 1.18$ and $Z_\chi \approx 0.48$, respectively, so that $Z_d \approx 0.57$. The limiting values $Z_d = 1$ for $U/t \rightarrow 0$ and $Z_d \approx 0.57$ for $U/t \rightarrow \infty$ and the approximate intermediate value,⁶ $Z_d \approx 0.65$, at $U/t = 8$ are recovered as solutions of the equation,

$$Z_d = e^{-Z_d \tanh(\sqrt{\frac{U}{4\pi t}})}, \quad (33)$$

which is used here for finite U/t .

The spin dynamical structure factor measured in the high-energy inelastic neutron scattering experiments of Ref. 2 includes a Bragg peak associated with its elastic part. The corresponding elastic spectral weight is included in the total spin-weight sum-rule, $\mu_B^2 2(1 - 2d)$, of Eq. (7). In the thermodynamic limit the upper-Hubbard band processes generate nearly no spin weight. Hence, the longitudinal spectral weight within the sum rule $\mu_B^2 2(1 - 2d)$ refers to the elastic contribution. The elastic weight is given by $\approx \mu_B^2 4(m_{AF})^2$. The inelastic spin spectral weight corresponds to the remaining weight in the spin-weight sum rule $\approx \mu_B^2 [2(1 - 2d) - 4(m_{AF})^2]$. It refers to the $-+$ spin dynamical structure factor given in Eq. (5) for $\alpha = -$ and $\alpha' = +$. It then follows that the experimentally determined spin-wave intensity, which corresponds to the coherent part of the inelastic spin spectral weight, is in units of μ_B^2 approximately given by

$$W_{SW} \approx Z_d [2(1 - 2d) - 4(m_{AF})^2]. \quad (34)$$

The GA + RPA method used in Ref. 6 accounts for the quantum fluctuations that control the longitudinal and transverse relative weights. Within our description notations, that method is designed to make the inelastic spin spectral weight $\mu_B^2 [2(1 - 2d) - 4(m_{AF})^2]$ rather than $\mu_B^2 2(1 - 2d)$. Hence, for that GA + RPA method the spin-wave intensity factor is Z_d as defined in Eq. (32).

On the other hand, the RPA used here refers to the $-+$ spin dynamical structure factor alone. Hence, it implicitly considers that the total inelastic spin spectral weight is $\mu_B^2 2(1 - 2d)$ rather than $\mu_B^2 [2(1 - 2d) - 4(m_{AF})^2]$. Therefore, to describe

the actual spin-wave intensity momentum distribution one must use a corresponding experimentally determined factor $Z_d^{\text{exp}} < Z_d$ such that

$$W_{SW} = Z_d^{\text{exp}} 2(1 - 2d) = Z_d [2(1 - 2d) - 4(m_{AF})^2]. \quad (35)$$

From the residue of the spin-wave pole the susceptibility coherent part then reads

$$\chi_{co}^{-+}(\vec{k}, i\omega) = Z_d^{\text{exp}} \sum_{l=\pm 1} \frac{\text{Res}[\chi^{-+}(\vec{k}, l\omega(\vec{k}))]}{i\omega - l\omega(\vec{k})}, \quad (36)$$

with χ^{-+} obtained in RPA above. The measured intensity is²⁷

$$I_{SW}(\vec{k}) = \pi[S^{xx}(\vec{k}) + S^{yy}(\vec{k})] = \pi S^{-+}(\vec{k}). \quad (37)$$

In Fig. 2 (bottom), we plot the corresponding RPA spin-wave intensity,

$$I_{SW}(\vec{k}) = -[\pi/2]Z_d^{\text{exp}} \text{Res}[\chi^{-+}(\vec{k}, \omega(\vec{k}))]. \quad (38)$$

The good agreement with the experimental data, specially near the point M , reproduces the theoretical results of Ref. 2. It is here obtained for the value $Z_d^{\text{exp}} \approx 0.49$, which corresponds to the choice $m_{AF} = m_{AF}^{GB} = m_{AF}^0(1 - 2d)$ such that $\delta S \approx d$. The m_{AF}^{GB} dependence on U/t is given in Eq. (22) for $U/t < 8$. As in Ref. 2, the spin-wave intensity shows disagreement around the X point, which here probably stems from effects not captured by the RPA.

V. THE ROTATED-ELECTRON DESCRIPTION EMERGING FROM THE MODEL'S EXTENDED GLOBAL SYMMETRY

The goal of this section is the introduction of the general rotated-electron representation from which the spinon representation used in the ensuing section naturally emerges. In contrast to the remaining sections of this paper, here we consider arbitrary values of the electronic density $n = N/N_a$ and spin density $m = [N_\uparrow - N_\downarrow]$.

A. The electron-rotated-electron unitary operator

We denote the spin and η -spin of an energy eigenstate by S_s and S_η , respectively. The corresponding spin and η -spin projections read $S_s^z = -\frac{1}{2}[N_\uparrow - N_\downarrow]$ and $S_\eta^z = -\frac{1}{2}[N_a - N]$, respectively. The lowest-weight states (LWSs) of both the η -spin and spin algebras are such that $S_\alpha = -S_\alpha^z$, where $\alpha = \eta$ for η spin and $\alpha = s$ for spin. The numbers

$$\begin{aligned} n_\eta &= S_\eta - \frac{1}{2}(N_a - N) = 0, 1, \dots, 2S_\eta, \\ n_s &= S_s - \frac{1}{2}(N_\uparrow - N_\downarrow) = 0, 1, \dots, 2S_s, \end{aligned} \quad (39)$$

vanish for such a LWS.

Let $\{|\Psi_{l_r, l_{\eta s}, u}\rangle\}$ be a complete set of 4^{N_a} energy, momentum, η -spin, η -spin projection, spin, and spin-projection eigenstates for $u \equiv U/t > 0$. Here $l_{\eta s}$ is a short notation for the set of four quantum numbers $[S_\eta, S_s, n_\eta, n_s]$ and the index l_r represents all remaining quantum numbers, other than those, that are needed to fully specify an energy eigenstate $|\Psi_{l_r, l_{\eta s}, u}\rangle$. The energy eigenstates of that set that are not LWSs are generated from

those as follows:

$$|\Psi_{l_r, l_{\eta s}, u}\rangle = \prod_{\alpha=\eta, s} \left[\frac{1}{\sqrt{C_\alpha}} (\hat{S}_\alpha^\dagger)^{n_\alpha} \right] |\Psi_{l_r, l_{\eta s}, u}^0\rangle. \quad (40)$$

Here,

$$\begin{aligned} C_\alpha &= \langle \Psi_{l_r, l_{\eta s}, u}^0 | (\hat{S}_\alpha)^{n_\alpha} (\hat{S}_\alpha^\dagger)^{n_\alpha} | \Psi_{l_r, l_{\eta s}, u}^0 \rangle \\ &= [n_\alpha!] \prod_{j'=1}^{n_\alpha} [2S_\alpha + 1 - j'], \quad \alpha = \eta, s, \end{aligned} \quad (41)$$

for $n_\alpha = 1, \dots, 2S_\alpha$ are normalization constants, the η -spin ($\alpha = \eta$) and spin ($\alpha = s$) off-diagonal generators \hat{S}_α^\dagger and \hat{S}_α are given in Eq. (A7) of Appendix A, and $l_{\eta s}$ and $l_{\eta s}^0$ stand for $[S_\eta, S_s, n_\eta, n_s]$ and $[S_\eta, S_s, 0, 0]$, respectively. Within our notation, $l_{\eta s}^0$ refers to values of the general index $l_{\eta s}$ associated with a LWS such that $n_\eta = n_s = 0$.

For the Hubbard model on the square lattice and also on the 1D lattice, upon adiabatically increasing U/t from any finite value to the $U/t \rightarrow \infty$ limit, each energy eigenstate $|\Psi_{l_r, l_{\eta s}, u}\rangle$ continuously evolves into a uniquely defined corresponding energy eigenstate $|\Psi_{l_r, l_{\eta s}, \infty}\rangle$, and vice versa. We emphasize though that, due to the high degeneracy among different spin sectors as well as η -spin sectors that occurs in the $U/t \rightarrow \infty$ limit, there are in such a limit many more choices of energy eigenstates sets than for U/t finite. Accordingly, upon adiabatically decreasing U/t most of such $U/t \rightarrow \infty$ states do not evolve into finite- U/t energy eigenstates. Our above procedure uniquely defines a convenient set of $U/t \rightarrow \infty$ energy eigenstates that upon adiabatically decreasing U/t do evolve into finite- U/t energy eigenstates.

Both the corresponding sets of 4^{N_a} states $\{|\Psi_{l_r, l_{\eta s}, u}\rangle\}$ and $\{|\Psi_{l_r, l_{\eta s}, \infty}\rangle\}$, respectively, are complete and refer to the same Hilbert space. Hence, there is a uniquely defined unitary transformation connecting the states $|\Psi_{l_r, l_{\eta s}, u}\rangle$ and $|\Psi_{l_r, l_{\eta s}, \infty}\rangle$. Indeed, since the model's Hilbert space is the same for all $U/t > 0$ values considered here, it follows from basic quantum-mechanics Hilbert-space and operator properties that for this choice there exists exactly one unitary operator $\hat{V} = \hat{V}(U/t)$ such that any $U/t \rightarrow \infty$ energy eigenstate $|\Psi_{l_r, l_{\eta s}, \infty}\rangle$ is transformed into the corresponding $U/t > 0$ energy eigenstate $|\Psi_{l_r, l_{\eta s}, u}\rangle$ as

$$|\Psi_{l_r, l_{\eta s}, u}\rangle = \hat{V}^\dagger |\Psi_{l_r, l_{\eta s}, \infty}\rangle. \quad (42)$$

The energy eigenstates $|\Psi_{l_r, l_{\eta s}, u}\rangle = \hat{V}^\dagger |\Psi_{l_r, l_{\eta s}, \infty}\rangle$ (one for each value of $U/t > 0$) that are generated from the same initial $U/t \rightarrow \infty$ energy eigenstate $|\Psi_{l_r, l_{\eta s}, \infty}\rangle$ belong to the same V tower.

The rotated-electron operators are given by

$$\begin{aligned} \tilde{c}_{\vec{r}_j, \sigma}^\dagger &= \hat{V}^\dagger c_{\vec{r}_j, \sigma}^\dagger \hat{V}; & \tilde{c}_{\vec{r}_j, \sigma} &= \hat{V}^\dagger c_{\vec{r}_j, \sigma} \hat{V}, \\ \tilde{n}_{\vec{r}_j, \sigma} &= \tilde{c}_{\vec{r}_j, \sigma}^\dagger \tilde{c}_{\vec{r}_j, \sigma}; & \hat{V} &= e^{-\hat{S}}. \end{aligned} \quad (43)$$

For $U/t > 0$ the operator \hat{S} appearing here can be expanded in a series of t/U whose leading-order term is provided in Eq. (A2) of Appendix A.

Since the electron-rotated-electron unitary operator \hat{V} commutes with itself, the equalities $\hat{V} = e^{-\hat{S}} = \tilde{V} = e^{-\tilde{S}}$ and $\hat{S} = \tilde{S}$ hold. Hence, both the operators \hat{V} and \tilde{S} have the same

expression in terms of electron and rotated-electron creation and annihilation operators. It then follows from the expression of the operator \hat{S} provided in Eq. (A2) of Appendix A that the corresponding rotated operator \tilde{S} has the following leading-order term,

$$\tilde{S} = -\frac{t}{U} [\tilde{T}_{+1} - \tilde{T}_{-1}] + \dots \quad (44)$$

The rotated kinetic operators \tilde{T}_{+1} and \tilde{T}_{-1} appearing here and the related rotated kinetic operator \tilde{T}_0 are given in Eq. (A3) of Appendix A. The expressions of the corresponding unrotated kinetic operators \hat{T}_0 , \hat{T}_{+1} , and \hat{T}_{-1} are provided in Eq. (A1) of that appendix.

Note that the equality $\hat{S} = \tilde{S}$ refers to the whole expression of these operators. An important property for our study is that except in the $U/t \rightarrow \infty$ limit the leading order terms $-\frac{t}{U} [\hat{T}_{+1} - \hat{T}_{-1}]$ and $-\frac{t}{U} [\tilde{T}_{+1} - \tilde{T}_{-1}]$ of the operators \hat{S} and \tilde{S} given in Eq. (A2) of Appendix A and Eq. (44), respectively, are different operators. Moreover, except for $U/t \rightarrow \infty$ one has that $\hat{T}_0 \neq \tilde{T}_0$, $\hat{T}_{+1} \neq \tilde{T}_{+1}$, and $\hat{T}_{-1} \neq \tilde{T}_{-1}$. This is behind for intermediate U/t values the few first terms of the Hamiltonian t/U expansion as written in terms of rotated-electron operators containing much more complicated higher-order terms when expressed in terms of electron creation and annihilation operators.

The main point here is that for the rotated electrons that emerge from the unitary transformation of Eq. (43) single and double occupancy are good quantum numbers for $U/t > 0$. Indeed, on any bipartite lattice the number of rotated-electron singly occupied sites operator,

$$2\tilde{S}_c = \hat{V}^\dagger \hat{Q} \hat{V} = \sum_{j=1}^{N_a} \tilde{s}_{\tilde{r}_j,c}, \quad (45)$$

$$\tilde{s}_{\tilde{r}_j,c} = \hat{V}^\dagger \hat{s}_{\tilde{r}_j,c} \hat{V} = \sum_{\sigma=\uparrow,\downarrow} \tilde{n}_{\tilde{r}_j,\sigma} (1 - \tilde{n}_{\tilde{r}_j,-\sigma}),$$

commutes with the Hubbard model Hamiltonian.¹⁴ Here \hat{Q} is the corresponding number of electron singly occupied sites operator given in Eq. (2). This follows in part from the symmetries of the Hamiltonian electron-interaction term, which imply that all $U/t \rightarrow \infty$ energy eigenstates of the set $\{|\Psi_{l,r,l_{\eta s},\infty}\rangle\}$ are as well eigenstates of the electron double-occupancy operator \hat{D} and single-occupancy operator \hat{Q} provided in that equation. Hence, in the $U/t \rightarrow \infty$ limit the Hilbert space is classified in subspaces with different numbers of doubly occupied sites and each of the states $\{|\Psi_{l,r,l_{\eta s},\infty}\rangle\}$ is contained in only one of these subspaces. The same applies to the 4^{N_a} energy eigenstates of the set $\{|\Psi_{l,r,l_{\eta s},u}\rangle\}$ for $U/t > 0$ in terms of rotated-electron doubly occupied sites.

The unitary operator \hat{V} of our formulation is uniquely defined by its $4^{N_a} \times 4^{N_a}$ matrix elements, $\langle \Psi_{l,r,l_{\eta s},u} | \hat{V} | \Psi_{l',r',l'_{\eta s},u} \rangle$. For $U/t > 0$ most of these matrix elements vanish. For $U/t \rightarrow \infty$ rotated electrons become electrons so that the matrix representing the unitary operator \hat{V} becomes the $4^{N_a} \times 4^{N_a}$ unit matrix. Hence, $\langle \Psi_{l,r,l_{\eta s},\infty} | \hat{V} | \Psi_{l',r',l'_{\eta s},\infty} \rangle = \delta_{l,r,l'} \delta_{l_{\eta s},l'_{\eta s}}$. On the other hand, as justified in Appendix A, the unitary operator $\hat{V} = \hat{V}(U/t)$ commutes with the six generators of the global η -spin and spin $SU(2)$ symmetries. This implies that the matrix elements between energy eigenstates with different values of

S_η , S_s , n_η , and n_s and thus of $l_{\eta s}$ vanish. Hence, the finite matrix elements are between states with the same $l_{\eta s}$ values so that we denote them by $V_{l,r,l'}$,

$$\langle \Psi_{l,r,l_{\eta s},\infty} | \hat{V} | \Psi_{l',r',l'_{\eta s},\infty} \rangle = \delta_{l_{\eta s},l'_{\eta s}} V_{l,r,l'}, \quad (46)$$

where

$$V_{l,r,l'} = \langle \Psi_{l,r,l_{\eta s},u} | \hat{V} | \Psi_{l',r',l'_{\eta s},u} \rangle = \langle \Psi_{l',r',l'_{\eta s},\infty} | \hat{V}^\dagger | \Psi_{l,r,l_{\eta s},\infty} \rangle^* \\ = \langle \Psi_{l,r,l_{\eta s},u} | \Psi_{l',r',l'_{\eta s},\infty} \rangle = \langle \Psi_{l',r',l'_{\eta s},\infty} | \Psi_{l,r,l_{\eta s},u} \rangle^*. \quad (47)$$

Given a complete set of 4^{N_a} energy, momentum, η -spin, η -spin projection, spin, and spin-projection eigenstates, $\{|\Psi_{l,r,l_{\eta s},u}\rangle\}$, the electron-rotated-electron unitary operator considered here is for $U/t > 0$ uniquely defined by the matrix elements of Eqs. (46) and (47). This corresponds to one out of the infinite choices of electron-rotated-electron unitary operators.¹⁴ All these operators and corresponding unitary transformations refer to the same subspaces with fixed numbers of doubly occupied sites, $0, 1, 2, 3, \dots$. They differ only in the choice of basis states within each of these subspaces. For most of these unitary operators the states $\hat{V}^\dagger |\Psi_{l,r,l_{\eta s},\infty}\rangle$ are not energy eigenstates for finite U/t values. The electron-rotated-electron unitary transformation considered here has been constructed to make these states energy eigenstates for finite U/t values, as given in Eq. (42).

B. The general operational description naturally emerging from the rotated electrons and symmetry

The electron-rotated-electron unitary transformation is closely related to the extended global $SO(3) \times SO(3) \times U(1)$ symmetry found in Ref. 14 for the Hamiltonian given in Eq. (1) on any bipartite lattice. Until recently¹⁸ it was believed that the model's global symmetry was for finite on-site interaction values only $SO(4) = [SU(2) \otimes SU(2)]/Z_2$. The occurrence of a global c hidden $U(1)$ symmetry beyond $SO(4)$ in the model's global $SO(3) \otimes SO(3) \otimes U(1) = [SO(4) \otimes U(1)]/Z_2$ symmetry must be accounted for in studies of the Hubbard model on any bipartite lattice. Such a global symmetry may be rewritten as $[SU(2) \times SU(2) \times U(1)]/Z_2^2$ and stems from the $U \neq 0$ local gauge $SU(2) \times SU(2) \times U(1)$ symmetry of the Hubbard model on a bipartite lattice with vanishing transfer integral, $t = 0$.¹⁹ The seven local generators of the corresponding two gauge $SU(2)$ symmetries and $U(1)$ symmetry are the three spin local operators $\hat{s}_{\tilde{r}_j,s}^z$ provided in Eq. (4) and the three η -spin local operators $\hat{s}_{\tilde{r}_j,\eta}^z$ and the local operator $\hat{s}_{\tilde{r}_j,c}$ given in Eqs. (A8) and (A9) of Appendix A, respectively. The index l in the generators of the two $SU(2)$ symmetries stand for $l = \pm, z$.

An important point is that although addition of chemical-potential and magnetic-field operator terms to the Hubbard model on a square lattice Hamiltonian given in Eq. (1) lowers its symmetry, these terms commute with it. Therefore, the global symmetry of the latter Hamiltonian being $SO(3) \otimes SO(3) \otimes U(1)$ implies that the set of independent rotated-electron occupancy configurations that generate all 4^{N_a} energy eigenstates, $\{|\Psi_{l,r,l_{\eta s},u}\rangle\}$, generate as well representations of the global symmetry algebra for all values of electronic density n and spin density m . It is confirmed in Ref. 14 that the number

of these independent $[\text{SU}(2) \otimes \text{SU}(2) \otimes \text{U}(1)]/Z_2^2 = \text{SO}(3) \otimes \text{SO}(3) \otimes \text{U}(1)$ symmetry algebra representations equals for the present model on a bipartite lattice its Hilbert-space dimension, 4^{N_a} .

The generator $\hat{s}_{\vec{r}_j,c}$ of the local gauge U(1) symmetry given in Eq. (A9) of Appendix A and the alternative local generator $\hat{s}_{\vec{r}_j,c}^h = (1 - \hat{s}_{\vec{r}_j,c})$ may be expressed as

$$\hat{s}_{\vec{r}_j,c} = \hat{q}_{\vec{r}_j}^c \equiv \hat{f}_{\vec{r}_j,c}^\dagger \hat{f}_{\vec{r}_j,c}, \quad \hat{s}_{\vec{r}_j,c}^h = (1 - \hat{q}_{\vec{r}_j}^c) = \hat{f}_{\vec{r}_j,c} \hat{f}_{\vec{r}_j,c}^\dagger. \quad (48)$$

Here $\hat{f}_{\vec{r}_j,c}^\dagger$ and $\hat{f}_{\vec{r}_j,c}$ stand for the following creation and annihilation operators, respectively, of suitable spinless and η -spinless fermions:

$$\begin{aligned} \hat{f}_{\vec{r}_j,c}^\dagger &= c_{\vec{r}_j,\uparrow}^\dagger (1 - \hat{n}_{\vec{r}_j,\downarrow}) + e^{i\vec{\pi}\cdot\vec{r}_j} c_{\vec{r}_j,\uparrow} \hat{n}_{\vec{r}_j,\downarrow}, \\ \hat{f}_{\vec{r}_j,c} &= c_{\vec{r}_j,\uparrow} (1 - \hat{n}_{\vec{r}_j,\downarrow}) + e^{i\vec{\pi}\cdot\vec{r}_j} c_{\vec{r}_j,\uparrow}^\dagger \hat{n}_{\vec{r}_j,\downarrow}, \end{aligned} \quad (49)$$

where we used that $e^{i\vec{\pi}\cdot\vec{r}_j} = e^{-i\vec{\pi}\cdot\vec{r}_j}$. Here and throughout this paper the vector $\vec{\pi}$ has Cartesian components $\vec{\pi} = [\pi, \pi]$.

We call *c fermions* the rotated-electron related objects whose creation and annihilation operators $f_{\vec{r}_j,c}^\dagger = \hat{V}^\dagger \hat{f}_{\vec{r}_j,c}^\dagger \hat{V}$ and $f_{\vec{r}_j,c} = \hat{V} \hat{f}_{\vec{r}_j,c} \hat{V}^\dagger$, respectively, are generated from those of the spinless and η -spinless fermions of Eq. (49) by the specific electron-rotated-electron unitary transformation uniquely defined by the matrix elements of Eqs. (46) and (47). [No upper index \hat{f} is used with the (rotated) *c* fermion operator $f_{\vec{r}_j,c}$.] Hence, these operators read

$$\begin{aligned} f_{\vec{r}_j,c}^\dagger &= \tilde{c}_{\vec{r}_j,\uparrow}^\dagger (1 - \tilde{n}_{\vec{r}_j,\downarrow}) + e^{i\vec{\pi}\cdot\vec{r}_j} \tilde{c}_{\vec{r}_j,\uparrow} \tilde{n}_{\vec{r}_j,\downarrow}, \\ f_{\vec{r}_j,c} &= \tilde{c}_{\vec{r}_j,\uparrow} (1 - \tilde{n}_{\vec{r}_j,\downarrow}) + e^{i\vec{\pi}\cdot\vec{r}_j} \tilde{c}_{\vec{r}_j,\uparrow}^\dagger \tilde{n}_{\vec{r}_j,\downarrow}. \end{aligned} \quad (50)$$

The rotated-electron creation and annihilation operators appearing here are generated from corresponding electron operators by the unitary transformation uniquely defined above, as given in Eq. (43). The corresponding *c* fermion local density operator is given by

$$\tilde{q}_{\vec{r}_j}^c = f_{\vec{r}_j,c}^\dagger f_{\vec{r}_j,c}. \quad (51)$$

The *c* fermions live on a lattice identical to the original lattice. One can introduce *c* fermion momentum dependent operators^{7,13}:

$$f_{\vec{q}_j,c}^\dagger = \frac{1}{\sqrt{N_a}} \sum_{j'=1}^{N_a} e^{+i\vec{q}_j\cdot\vec{r}_{j'}} f_{\vec{r}_{j'},c}^\dagger; \quad j = 1, \dots, N_a. \quad (52)$$

Here the *c* fermion operators $f_{\vec{q}_j,c}^\dagger$ where the index $j' = 1, \dots, N_a$ refers to the sites of the original lattice are mapped from the rotated-electron operators by an exact local transformation given in Eq. (50). The *c* momentum band has N_a discrete momentum values \vec{q}_j , where $j = 1, \dots, N_a$. It has the same shape and momentum area as the electronic first BZ.

The generator $2\tilde{S}_c$ of the related global *c* hidden U(1) symmetry in $[\text{SU}(2) \times \text{SU}(2) \times \text{U}(1)]/Z_2^2$ found in Ref. 14 is the number of rotated-electron singly occupied sites given in Eq. (45). Hence, it involves the site summation $\sum_{j=1}^{N_a}$ over the rotated local generator $\tilde{s}_{\vec{r}_j,c}$ rather than over the corresponding unrotated local operator $\hat{s}_{\vec{r}_j,c}$ of Eq. (A9) of Appendix A. This

is why $2\tilde{S}_c = \hat{V}^\dagger \hat{Q} \hat{V}$, as given in Eq. (45), where the operator \hat{Q} is that of Eq. (2). The eigenvalues $2S_c = 0, 1, 2, \dots$, of the generator $2\tilde{S}_c$ are thus the numbers of rotated-electron singly occupied sites.

The *c* fermion creation and annihilation operators are found in Appendix A to obey the anticommutation relations given in Eq. (A10) of that appendix. A straightforward operator algebra then confirms that the *c* fermion local density operator of Eq. (51) is the local operator $\tilde{s}_{\vec{r}_j,c}$ appearing in the expression provided in Eq. (45). Hence, the global *c* hidden U(1) symmetry generator may be simply rewritten as

$$2\tilde{S}_c = \sum_{j=1}^{N_a} \tilde{q}_{\vec{r}_j}^c = \sum_{j=1}^{N_a} f_{\vec{r}_j,c}^\dagger f_{\vec{r}_j,c}. \quad (53)$$

One finds that except in the $U/t \rightarrow \infty$ limit the inequality $\sum_{j=1}^{N_a} \hat{q}_{\vec{r}_j}^c \neq \sum_{j=1}^{N_a} \tilde{q}_{\vec{r}_j}^c$ holds. This confirms that the generator $2\tilde{S}_c$ given in Eq. (53) does not commute with the electron-rotated-electron unitary operator $\hat{V} = \hat{V}$. On the other hand, and as justified in Appendix A, the three components of the momentum operator \hat{P} , three generators of the global spin SU(2) symmetry, and three generators of the global η -spin SU(2) symmetry commute with that unitary operator. Hence, in contrast to the Hamiltonian and generator $2\tilde{S}_c$, these operators have the same expression in terms of electron and rotated-electron creation and annihilation operators, as given in Eqs. (A6) and (A7) of Appendix A. On the contrary, the generator of the global *c* hidden U(1) symmetry given in Eq. (45) does not commute with the unitary operator \hat{V} . This is behind the hidden character of such a symmetry.

Site summation $\sum_{j=1}^{N_a}$ over the rotated local operator provided in Eq. (51) and over the following six rotated local operators,

$$\begin{aligned} \tilde{s}_{\vec{r}_j,\eta}^z &= -\frac{1}{2} [1 - \tilde{n}_{\vec{r}_j,\uparrow} - \tilde{n}_{\vec{r}_j,\downarrow}], \\ \tilde{s}_{\vec{r}_j,\eta}^+ &= e^{i\vec{\pi}\cdot\vec{r}_j} \tilde{c}_{\vec{r}_j,\downarrow}^\dagger \tilde{c}_{\vec{r}_j,\uparrow}^\dagger, \quad \tilde{s}_{\vec{r}_j,\eta}^- = e^{-i\vec{\pi}\cdot\vec{r}_j} \tilde{c}_{\vec{r}_j,\uparrow} \tilde{c}_{\vec{r}_j,\downarrow}, \\ \tilde{s}_{\vec{r}_j,s}^z &= -\frac{1}{2} [\tilde{n}_{\vec{r}_j,\uparrow} - \tilde{n}_{\vec{r}_j,\downarrow}], \quad \tilde{s}_{\vec{r}_j,s}^+ = \tilde{c}_{\vec{r}_j,\downarrow}^\dagger \tilde{c}_{\vec{r}_j,\uparrow}^\dagger, \\ \tilde{s}_{\vec{r}_j,s}^- &= \tilde{c}_{\vec{r}_j,\uparrow} \tilde{c}_{\vec{r}_j,\downarrow}, \quad j = 1, 2, \dots, N_a, \end{aligned} \quad (54)$$

gives the seven generators of the model's global $\text{SO}(3) \otimes \text{SO}(3) \otimes \text{U}(1) = [\text{SU}(2) \otimes \text{SU}(2) \otimes \text{U}(1)]/Z_2^2$ symmetry, as provided in Eqs. (45) and (A7) of Appendix A. However, except in the $U/t \rightarrow \infty$ limit the six rotated local operators given in Eq. (54) and the corresponding six unrotated local operators provided in Eqs. (4) and (A8) of Appendix A are different operators.

Interestingly, the η -spin and spin SU(2) symmetries are within the present representation particular cases of a general ηs quasispin SU(2) symmetry. The corresponding three local ηs quasispin operators $\tilde{q}_{\vec{r}_j}^l$ such that $l = \pm, z$ obey a SU(2) algebra and have the following expression in terms of rotated-electron operators,

$$\begin{aligned} \tilde{q}_{\vec{r}_j}^- &= (\tilde{c}_{\vec{r}_j,\uparrow}^\dagger + e^{i\vec{\pi}\cdot\vec{r}_j} \tilde{c}_{\vec{r}_j,\uparrow}) \tilde{c}_{\vec{r}_j,\downarrow}, \\ \tilde{q}_{\vec{r}_j}^+ &= (\tilde{q}_{\vec{r}_j}^-)^\dagger; \quad \tilde{q}_{\vec{r}_j}^z = (\tilde{n}_{\vec{r}_j,\downarrow} - 1/2). \end{aligned} \quad (55)$$

Here $\tilde{q}_{\vec{r}_j}^\pm = \tilde{q}_{\vec{r}_j}^x \pm i \tilde{q}_{\vec{r}_j}^y$, where x, y, z denotes the Cartesian coordinates. The relation of these η s quasispin operators to the original electron creation and annihilation operators involves the unitary transformation of Eq. (43).

Within the present rotated-electron operational formulation, three related elementary objects naturally emerge that make the model's global symmetry explicit. The operators provided in Eq. (50) create and annihilate spinless and η -spinless c fermions whose local density operator [Eq. (51)] is directly related to the generator of the global c hidden $U(1)$ symmetry, as given in Eq. (53). The c fermions carry the charges of the rotated electrons that singly occupy sites. Moreover, the three rotated local spin operators $\tilde{s}_{\vec{r}_j, s}^l$ and the three rotated local η -spin operators $\tilde{s}_{\vec{r}_j, \eta}^l$ such that $l = \pm, z$ given in Eq. (54) are associated with the spin- $\frac{1}{2}$ spinons and η -spin- $\frac{1}{2}$ η spinons, respectively, as defined here. The spin- $\frac{1}{2}$ spinons carry the spin of the rotated electrons that singly occupy sites. The c fermion holes describe the degrees of freedom associated with the c hidden $U(1)$ symmetry of the sites doubly occupied and unoccupied by the rotated electrons. The η -spin degrees of freedom of these sites are described by the η -spin projection $-1/2$ η spinons (rotated-electron doubly occupied sites) and η -spin projection $+1/2$ η spinons (rotated-electron unoccupied sites).

Within our representation, the local operators $\tilde{s}_{\vec{r}_j, c}^h$, $\tilde{s}_{\vec{r}_j, c}^h$, and $\tilde{s}_{\vec{r}_j, \alpha}^l$, where $l = \pm, z$ and $\alpha = s, \eta$ can be expressed in terms of only the c fermion local density operator $\tilde{q}_{\vec{r}_j}^c$ given in Eq. (51) and three local η s quasispin operators $\tilde{q}_{\vec{r}_j}^l$ of Eq. (55) as follows:

$$\begin{aligned} \tilde{s}_{\vec{r}_j, c} &= \tilde{q}_{\vec{r}_j}^c; & \tilde{s}_{\vec{r}_j, c}^h &= (1 - \tilde{q}_{\vec{r}_j}^c), \\ \tilde{s}_{\vec{r}_j, s}^l &= \tilde{q}_{\vec{r}_j}^c \tilde{q}_{\vec{r}_j}^l; & \tilde{s}_{\vec{r}_j, \eta}^l &= (1 - \tilde{q}_{\vec{r}_j}^c) \tilde{q}_{\vec{r}_j}^l, \quad l = \pm, z. \end{aligned} \quad (56)$$

The expressions of the local spinon operators $\tilde{s}_{\vec{r}_j, s}^l$ and local η -spinon operators $\tilde{s}_{\vec{r}_j, \eta}^l$ provided here are a confirmation that the corresponding spin $SU(2)$ and η -spin $SU(2)$ symmetries are particular cases of the η s quasispin $SU(2)$ symmetry. Specifically, they are associated with the $SU(2)$ algebra representations involving the (i) spin-up and spin-down rotated-electron singly occupied sites and (ii) rotated-electron doubly occupied and unoccupied sites, respectively. Indeed, the c fermion and c fermion hole local density operators $\tilde{q}_{\vec{r}_j}^c$ and $(1 - \tilde{q}_{\vec{r}_j}^c)$ play in the expressions of these operators provided in Eq. (56) the role of projectors onto such two sets of lattice-site rotated-electron occupancies, respectively.

The relations given in Eq. (56) for the operators $\tilde{s}_{\vec{r}_j, s}^l$ and $\tilde{s}_{\vec{r}_j, \eta}^l$ are equivalent to the following expression of the local η s quasispin operators $\tilde{q}_{\vec{r}_j}^l$ in terms of those of the former operators provided in Eq. (54),

$$\tilde{q}_{\vec{r}_j}^l = \tilde{s}_{\vec{r}_j, s}^l + \tilde{s}_{\vec{r}_j, \eta}^l, \quad l = \pm, z. \quad (57)$$

We emphasize that the c fermion operators [Eq. (50)] and the spinon and η -spinon operators defined by Eqs. (54)–(56) are mapped from the rotated-electron operators by an exact local unitary transformation that does not introduce constraints.

Given their direct relation to the generators of the model's extended global symmetry, their occupancy configurations naturally generate representations of the corresponding global symmetry algebra. Consistent with the lack of constraints of such a local unitary transformation, inversion of the relations given in Eqs. (50) and (55) fully defines the rotated-electron operators in terms of the c fermion and η s quasispin operators as follows:

$$\begin{aligned} \tilde{c}_{\vec{r}_j, \uparrow}^\dagger &= f_{\vec{r}_j, c}^\dagger \left(\frac{1}{2} - \tilde{q}_{\vec{r}_j}^z \right) + e^{i\vec{\pi} \cdot \vec{r}_j} f_{\vec{r}_j, c} \left(\frac{1}{2} + \tilde{q}_{\vec{r}_j}^z \right), \\ \tilde{c}_{\vec{r}_j, \downarrow}^\dagger &= (f_{\vec{r}_j, c}^\dagger + e^{i\vec{\pi} \cdot \vec{r}_j} f_{\vec{r}_j, c}) \tilde{q}_{\vec{r}_j}^+, \\ \tilde{c}_{\vec{r}_j, \uparrow} &= f_{\vec{r}_j, c} \left(\frac{1}{2} - \tilde{q}_{\vec{r}_j}^z \right) + e^{i\vec{\pi} \cdot \vec{r}_j} f_{\vec{r}_j, c}^\dagger \left(\frac{1}{2} + \tilde{q}_{\vec{r}_j}^z \right), \\ \tilde{c}_{\vec{r}_j, \downarrow} &= (f_{\vec{r}_j, c} + e^{i\vec{\pi} \cdot \vec{r}_j} f_{\vec{r}_j, c}^\dagger) \tilde{q}_{\vec{r}_j}^-. \end{aligned} \quad (58)$$

As given in Eq. (A11) of Appendix A that the c fermion operators commute with the η s quasispin operators is behind the form of the expressions given here, whose c fermion creation and annihilation operators are located on the left-hand side.

The c fermion operator and η s quasispin operator expressions in terms of rotated-electron creation and annihilation operators given in Eqs. (50) and (55), respectively, are, except for unimportant phase factors, similar to those considered in the studies of Refs. 28–30 in terms of electron creation and annihilation operators. Our operational representation has the advantage of rotated-electron single and double occupancy being good quantum numbers for all finite interaction values. On the other hand, the operator expressions provided in Eqs. (50) and (55) differ from those of Refs. 7 and 13 by unimportant phase factors.

Since for finite U/t values the Hamiltonian \hat{H} of Eq. (1) does not commute with the unitary operator $\hat{V} = e^{-\hat{S}}$, when expressed in terms of the rotated-electron creation and annihilation operators of Eq. (43) it has an infinite number of terms,

$$\hat{H} = \hat{V} \tilde{H} \hat{V}^\dagger = \tilde{H} + [\tilde{H}, \tilde{S}] + \frac{1}{2} [[\tilde{H}, \tilde{S}], \tilde{S}] + \dots \quad (59)$$

The commutator $[\tilde{H}, \tilde{S}]$ does not vanish except for $U/t \rightarrow \infty$ so that $\hat{H} \neq \tilde{H}$ for finite values of U/t .

Provided that both U/t is finite and one accounts for all higher-order terms on the right-hand-side of Eq. (59), the corresponding expression refers to the Hubbard model. This is in contrast to the physical problem studied in Refs. 31–34, for which the rotated creation and annihilation operators of Eq. (43) refer to electrons. Thus, except for $U/t \rightarrow \infty$ within the physical problem studied in Refs. 31–34 the Hamiltonian given in Eq. (59) is not the Hubbard Hamiltonian. Instead, it is a rotated Hamiltonian for which electron double occupancy and single occupancy are good quantum numbers. On the other hand, for the alternative physical problem studied here and in Refs. 7 and 13 the rotated creation and annihilation operators of Eq. (43) refer to rotated electrons and the Hamiltonian provided in Eq. (59) is the Hubbard Hamiltonian.

The latter Hamiltonian may be developed into an expansion whose terms can be written as products of the rotated kinetic operators \tilde{T}_γ given in Eq. (A3) of Appendix A where $\gamma = 0, \pm 1$. The corresponding order of a given Hamiltonian term refers to the number of such rotated kinetic operators \tilde{T}_γ independently of their type, $\gamma = 0, \pm 1$. To fourth order such

a Hamiltonian reads

$$\begin{aligned}\hat{H} &= \hat{H}^{(0)} + \hat{H}^{(1)} + \hat{H}^{(2)} + \hat{H}^{(3)} + \hat{H}^{(4)} + \dots, \\ \hat{H}^{(0)} &= U \tilde{V}_D; \quad \hat{H}^{(1)} = t \tilde{T}_0, \quad \hat{H}^{(2)} = -\frac{t^2}{U} \tilde{T}_{-1} \tilde{T}_{+1}, \\ \hat{H}^{(3)} &= \frac{t^3}{U^2} \left[\tilde{T}_{-1} \tilde{T}_0 \tilde{T}_{+1} - \frac{1}{2} (\tilde{T}_{-1} \tilde{T}_{+1} \tilde{T}_0 + \tilde{T}_0 \tilde{T}_{-1} \tilde{T}_{+1}) \right], \\ \hat{H}^{(4)} &= \frac{t^4}{U^3} \left[\tilde{T}_{-1} \tilde{T}_0 \tilde{T}_{+1} \tilde{T}_0 + \tilde{T}_0 \tilde{T}_{-1} \tilde{T}_0 \tilde{T}_{+1} - \tilde{T}_{-1} \tilde{T}_0^2 \tilde{T}_{+1} \right. \\ &\quad - \frac{1}{2} \tilde{T}_{-1}^2 \tilde{T}_{+1}^2 + \tilde{T}_{-1} \tilde{T}_{+1} \tilde{T}_{-1} \tilde{T}_{+1} \\ &\quad - \frac{1}{2} (\tilde{T}_{-1} \tilde{T}_{+1} \tilde{T}_0^2 + \tilde{T}_0^2 \tilde{T}_{-1} \tilde{T}_{+1}) \\ &\quad \left. + \theta (2 \tilde{T}_0 \tilde{T}_{-1} \tilde{T}_{+1} \tilde{T}_0 - \tilde{T}_{-1} \tilde{T}_{+1} \tilde{T}_0^2 - \tilde{T}_0^2 \tilde{T}_{-1} \tilde{T}_{+1}) \right], \\ \theta, \quad &\text{real-number parameter.} \quad (60)\end{aligned}$$

Here,

$$\tilde{V}_D = \hat{V}^\dagger \hat{V}_D \hat{V} = \sum_{j=1}^{N_a} (\tilde{n}_{\tilde{r}_j, \uparrow} - 1/2)(\tilde{n}_{\tilde{r}_j, \downarrow} - 1/2) \quad (61)$$

is the rotated-electron interaction operator. That it appears only once in the Hamiltonian expansion whose leading-order terms are given in Eq. (60) follows from the derivation of that expansion systematically using the commutator,

$$[\tilde{V}_D, \tilde{T}_\gamma] = \gamma \tilde{T}_\gamma, \quad \gamma = 0, \pm 1. \quad (62)$$

We recall that except for $U/t \rightarrow \infty$ one has that $\hat{T}_0 \neq \tilde{T}_0$, $\hat{T}_{+1} \neq \tilde{T}_{+1}$, and $\hat{T}_{-1} \neq \tilde{T}_{-1}$. Expressing the Hamiltonian expression of Eq. (60) in terms of electron creation and annihilation operators gives for large U/t values a similar expansion. However, for the intermediate U/t values of interest for our study the few first terms of the Hamiltonian t/U expansion given in of Eq. (60) in terms of rotated-electron operators contain much more complicated higher-order terms when expressed in terms of electron creation and annihilation operators.

That Hamiltonian expansion may be expressed in terms of the c fermion and η_S quasispin operators. This is achieved by combining the rotated-electron operator expressions provided in Eq. (58) with those of the rotated-electron interaction operator given in Eq. (61) and three rotated kinetic operators \tilde{T}_0 , \tilde{T}_{-1} , and \tilde{T}_{+1} provided in Eq. (A3) of Appendix A.

If a rotated-electron term of an operator expansion in terms of rotated-electron creation and annihilation operators does not preserve the numbers of rotated-electron singly and doubly occupied sites, we call it off-diagonal. An interesting technical detail is that up to third order all diagonal terms of the Hamiltonian expression provided in Eq. (60) are generated by the leading-order term of the operator \tilde{S} , which is given in Eq. (44). Indeed, when expressed in terms of electron operators the Hubbard Hamiltonian provided in Eq. (1) does not contain any off-diagonal terms with more than two electron operators. (In this case the off-diagonal terms are electron off-diagonal terms, which refer to electron doubly occupied sites.)

Only the Hamiltonian terms $\hat{H}^{(0)}$, $\hat{H}^{(1)}$, $\hat{H}^{(2)}$, and $\hat{H}^{(3)}$ to third order given in Eq. (60) are universal. Indeed, the

form of the terms of fourth and larger order is different for each electron-rotated-electron unitary transformation. For the fourth-order term $\hat{H}^{(4)}$ given in that equation only the real-number parameter θ value is not universal, being unitary-transformation dependent.³² For instance, the methods of Refs. 33 and 34 refer to two different electron-rotated-electron unitary transformations whose θ values are $\theta = 0$ and $\theta = 1/4$, respectively. Moreover, one of the methods of Ref. 32 refers to an electron-rotated-electron unitary transformation whose θ value is $\theta = 1/2$. Its value for the electron-rotated-electron unitary transformation whose unitary operator is uniquely defined by the matrix elements of Eqs. (46) and (47) remains an open issue. Fortunately, these Hamiltonian terms multiplying the parameter θ vanish at half filling so that this does not affect the ensuing section studies.

The nonuniversal Hamiltonian terms are all reducible with respect to the subspaces with fixed values of rotated-electron single and double occupancies. That is, they contain hopping processes that do not originate from excitation between these subspaces, $\tilde{T}_0 \tilde{T}_{-1} \tilde{T}_{+1} \tilde{T}_0$, nor terminate once a rotated electron or rotated hole is returned to a subspace with larger single occupancy, for example, $\tilde{T}_{-1} \tilde{T}_{+1} \tilde{T}_{-1} \tilde{T}_{+1}$. All these processes can be viewed as arising from the specific transformation $\hat{V}^\dagger |\Psi_{l, \eta_S, \infty}\rangle$ of the $U/t \rightarrow \infty$ energy eigenstates within the subspaces with fixed values of rotated-electron single and double occupancies. Thus, the infinite electron-rotated-electron unitary transformations differ in the processes within each subspace with fixed values of these occupancies.

VI. GENERAL $S_s = 1$ SPIN SPECTRUM WITHIN THE SPINON REPRESENTATION

As discussed in Sec. I, the usual spin-wave theory does not describe the neutron scattering of LCO. Here we study the $S_s = 1$ spin-triplet spectrum of the half-filled Hubbard model on the square lattice by means of the spinon representation that emerges from the above more general c fermion and η_S quasispin operator formulation, which is that suitable for the LCO intermediate interaction range $U/t \in (6, 8)$. [In units of the bandwidth, $8t$, this gives $U/8t \in (0.75, 1)$.]

For very large U/t values the Hubbard model may be mapped onto a spin-only problem whose spins are those of the electrons that singly occupy sites. However, for intermediate U/t values electron single occupancy is not a good quantum number so that such a mapping breaks down. On the other hand, the rotated electrons of our operator representation have been constructed to make rotated-electron single and double occupancy good quantum numbers for $U/t > 0$. This is why our spinons are well defined for the LCO intermediate interaction range $U/t \in (6, 8)$. Indeed, they are the spins of the rotated electrons that singly occupy sites. In the large- U/t limit the rotated-electrons become electrons, so that one recovers the known standard results.

Within our operator formulation, the Hubbard model in the vanishing rotated-electron doubly occupied sites number and unoccupied sites number subspace (VDU subspace) can be mapped onto a spin-only problem for all U/t finite values. In the VDU subspace the number of spin- $\frac{1}{2}$ spinons equals that of rotated electrons, electrons, and sites $N = N_a$. Since there are no rotated-electron doubly occupied or unoccupied sites,

there are no η spinons. Hence, the number of η -spin SU(2) symmetry algebra representations vanishes and that symmetry does not play any role. Furthermore, although there are $N = N_a$ c fermions, their c momentum band associated with the operators of Eq. (52) is full. Hence, the degrees of freedom associated with the c fermion occupancy configurations that generate the c hidden U(1) symmetry algebra representations are frozen and the Hubbard model in the subspace under consideration may be mapped onto a spin-only problem, as confirmed below.

For $U/t \rightarrow \infty$ the VDU subspace is the only one for finite excitation energy. For the finite- U/t spin excitations that preserve the electron number $N = N_a$ considered in the following, it is the only subspace within a finite excitation-energy window, $\omega \in (0, 2\Delta_{MH})$. Here $2\Delta_{MH}$ is the Mott-Hubbard gap. Below we calculate its U/t dependence for the LCO intermediate interaction range $U/t \in (6, 8)$ by DMRG. Our goal is to check whether the relevant spin energy spectrum that emerges from our VDU subspace spin-only problem is indeed contained in the excitation-energy domain $\omega \in (0, 2\Delta_{MH})$ for which it is valid.

A. The energy range of our spin-only quantum problem

From the interplay of the model's symmetries with our operator formulation that makes these symmetries explicit, one straightforwardly confirms that the minimum energy for creation of one rotated-electron doubly occupied site or one rotated-electron unoccupied site at fixed electron number $N = N_a$ onto the $n = 1$ and $m = 0$ ground state is indeed given by the Mott-Hubbard gap, $2\Delta_{MH}$. Its magnitude is twice that of the single-particle gap, Δ_{MH} . In order to define the energy range of our study, here we calculate the Mott-Hubbard gap $2\Delta_{MH}$ dependence on U/t for a domain containing the LCO range $U/t \in (6, 8)$.

Our DMRG calculations refer to the single-particle gap. They have been performed both for 10×4 and 10×6 Hubbard cylinders. The chemical potential was set to $U/2$ and two states were targeted, one with N particles and the other with $N - 1$. (Targeting $N + 1$ electrons would have given the same results.) Both states were put into the same density matrix in the traditional multistate targeting DMRG approach. Thus, the same truncation error applied to both states, leading to significant error cancellation. The resulting gap at each sweep was plotted versus the maximum truncation error in the sweep, yielding approximately linear behavior, and allowing the extrapolation to zero truncation error. The error estimate is roughly the size of the extrapolation from the last point. From 1800 (10×4 Hubbard cylinder) to 6000 (10×6 Hubbard cylinder) states were kept.

Here we report the corresponding magnitudes of the Mott-Hubbard gap $2\Delta_{MH}$. For the range $U/t \in (4, 20)$ we find that

$$2\Delta_{MH} \approx U \left[\tanh \left(\sqrt{\frac{U/\gamma t}{\sqrt{6}\gamma + \sqrt{U/\gamma t}}} \right) \right]^2; \quad \gamma = \frac{\pi + 6}{6}, \quad (63)$$

gives quantitative agreement with our numerical DMRG calculations for the Mott-Hubbard gap $2\Delta_{MH}$ dependence on

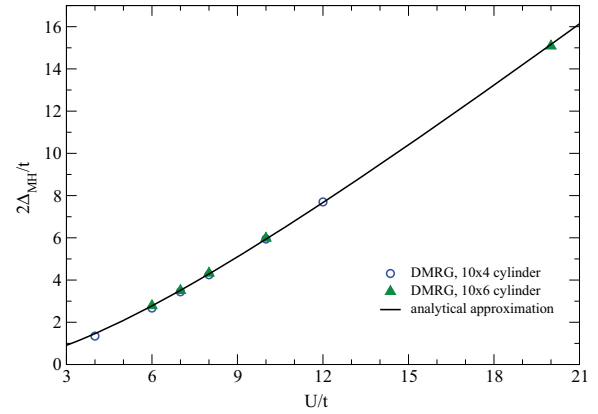


FIG. 3. (Color online) The Mott-Hubbard gap $2\Delta_{MH}$ DMRG numerical results on two different-width cylinders along with the approximate analytical expression of Eq. (63) (solid line) as a function of U/t . The DMRG points seem to be consistent with for the half-filled Hubbard on the square lattice the Mott-Hubbard gap being finite for $U/t > 0$ and vanishing in the $U/t \rightarrow 0$ limit.

U/t . The DMRG points for that gap are plotted in Fig. 3 along with the curve obtained from the approximate analytical expression [Eq. (63)].

For instance, our DMRG calculations for 10×6 Hubbard cylinders give $2\Delta_{MH} \approx 2.78(4)t$ for $U/t = 6$ and $\Delta_{MH} = 4.30(4)t$ for $U/t = 8$. This leads to a range $2\Delta_{MH} \in (816, 1442 \text{ meV})$ for $U/t \in (6, 8)$. Here we used the t magnitudes $t \approx 293 \text{ meV}$ and $t \approx 335 \text{ meV}$ for which the model describes the LCO neutron scattering for $U/t = 6$ and $U/t = 8$, respectively. For the $U/t = 6.1$ value used in some of our calculations, we find $\Delta_{MH} \approx 2.81(0)t$ from the DMRG analysis, so that $\Delta_{MH} \approx 829 \text{ meV}$ for $t \approx 295 \text{ meV}$.

Optical experiments overestimate the charge-transfer gap magnitudes of the parent insulating compounds.³⁵ On the other hand, by measuring the Hall coefficient R_H in LCO, the studies of Ref. 36 have estimated the energy gap over which the electron and hole carriers are thermally activated, which corresponds to the Mott-Hubbard gap, to be $2\Delta_{MH} \approx 890 \text{ meV}$. Remarkably, this magnitude is within the range $2\Delta_{MH} \in (816, 1442 \text{ meV})$ of our above theoretical predictions for $U/t \in (6, 8)$. Our theoretical approach based on the combination of our DMRG results with the U and t values for which agreement with the LCO neutron-scattering agreement is reached leads to $2\Delta_{MH} \approx 890 \text{ meV}$ for $U/t \approx 6.3$. Below we consistently confirm that the spin-triplet excitation spectrum calculated for the Hubbard model in the VDU subspace is contained in the energy window $\omega \in (0, 2\Delta_{MH})$ found here.

Note that the DMRG points of Fig. 3 seem to be consistent with the Mott-Hubbard gap being finite for $U/t > 0$ and vanishing in the $U/t \rightarrow 0$ limit.

B. The Hubbard model in the VDU subspace

Let us confirm that within our operator representation the half-filled Hubbard model on the square lattice in the VDU subspace can for $U/t > 0$ be expressed solely in terms of spinon operators. Indeed, accounting for the lack of both rotated-electron doubly occupied sites and unoccupied sites, upon writing the Hamiltonian of Eq. (60) in the VDU subspace, one finds that all its terms of odd order vanish and the terms

of even order given in that equation simplify to

$$\begin{aligned}\hat{H}^{(0)} &= U \tilde{V}^c, \quad \hat{H}^{(2)} = -\frac{t^2}{U} \tilde{T}_{-1} \tilde{T}_{+1}, \\ \hat{H}^{(4)} &= \frac{t^4}{U^3} \left[\tilde{T}_{-1} \tilde{T}_{+1} \tilde{T}_{-1} \tilde{T}_{+1} - \frac{1}{2} \tilde{T}_{-1}^2 \tilde{T}_{+1}^2 - \tilde{T}_{-1} \tilde{T}_0^2 \tilde{T}_{+1} \right].\end{aligned}\quad (64)$$

We have then expressed the Hamiltonian terms of even order as those provided in Eq. (64) in terms of the c fermion and η_s quasispin operators. This has been done by combining the rotated-electron operator expressions provided in Eq. (58) with those of the three rotated kinetic operators \tilde{T}_0 , \tilde{T}_{-1} , and \tilde{T}_{+1} given in Eq. (A3) of Appendix A. Since the states that span the VDU subspace are generated only by rotated-electron singly occupancy configurations, the projectors $\tilde{q}_{\vec{r}_j}^c$ and $(1 - \tilde{q}_{\vec{r}_j}^c)$ in the expressions of Eq. (56) can be replaced by the corresponding eigenvalues 1 and 0, respectively. One then finds that $\tilde{s}_{\vec{r}_j, s}^l = \tilde{q}_{\vec{r}_j}^l$ in the VDU subspace, so that the η -spin operators do not play any role. Hence, in it the η_s quasi-spin operators $\tilde{q}_{\vec{r}_j}^l$ reduce to the corresponding spinon operators $\tilde{s}_{\vec{r}_j, s}^l$, where $l = \pm, z$.

Moreover, after some algebra involving the anticommutation and commutation relations given in Eqs. (A10)–(A13) of Appendix A, one finds that all contributions involving the c fermion creation and annihilation operators can be expressed only in terms of local operators $\tilde{q}_{\vec{r}_j}^c$. In the VDU subspace one can then replace these operators by their eigenvalue 1. Thus, the Hamiltonian terms of Eq. (64) can be expressed only in terms of spinon operators. Importantly, this holds as well for the remaining Hamiltonian terms of higher even order omitted in that equation. Moreover, all Hamiltonian terms of odd order vanish and the zeroth-order term becomes a mere constant, $\hat{H}^{(0)} = [U/4] N_a$, and may be ignored. The Hamiltonian terms of second and fourth order of Eq. (64) may after some algebra then be rewritten as

$$\hat{H}^{(2)} = \frac{t^2}{U} \sum_{\langle j_1 j_2 \rangle} \frac{1}{2} [\tilde{s}_{\vec{r}_{j_1}, s} \cdot \tilde{s}_{\vec{r}_{j_2}, s} - 1], \quad (65)$$

and

$$\begin{aligned}\hat{H}^{(4)} &= -\frac{t^4}{U^3} \sum_{\langle j_1 j_2 \rangle} \frac{1}{2} [\tilde{s}_{\vec{r}_{j_1}, s} \cdot \tilde{s}_{\vec{r}_{j_2}, s} - 1] \\ &+ \frac{t^4}{U^3} \sum_{j_1, j_2, j_3} \frac{1}{2} D_{j_1, j_2} D_{j_2, j_3} [\tilde{s}_{\vec{r}_{j_1}, s} \cdot \tilde{s}_{\vec{r}_{j_3}, s} - 1] \\ &+ \frac{t^4}{U^3} \sum_{j_1, j_2, j_3, j_4} \frac{1}{8} D_{j_1, j_2} D_{j_2, j_3} D_{j_3, j_4} D_{j_4, j_1} \\ &\times [1 - \tilde{s}_{\vec{r}_{j_1}, s} \cdot \tilde{s}_{\vec{r}_{j_2}, s} - \tilde{s}_{\vec{r}_{j_1}, s} \cdot \tilde{s}_{\vec{r}_{j_3}, s} - \tilde{s}_{\vec{r}_{j_1}, s} \cdot \tilde{s}_{\vec{r}_{j_4}, s} \\ &- \tilde{s}_{\vec{r}_{j_2}, s} \cdot \tilde{s}_{\vec{r}_{j_3}, s} - \tilde{s}_{\vec{r}_{j_2}, s} \cdot \tilde{s}_{\vec{r}_{j_4}, s} - \tilde{s}_{\vec{r}_{j_3}, s} \cdot \tilde{s}_{\vec{r}_{j_4}, s}] \\ &+ \frac{t^4}{U^3} \sum_{j_1, j_2, j_3, j_4} \frac{5}{8} D_{j_1, j_2} D_{j_2, j_3} D_{j_3, j_4} D_{j_4, j_1} \\ &\times [(\tilde{s}_{\vec{r}_{j_1}, s} \cdot \tilde{s}_{\vec{r}_{j_2}, s})(\tilde{s}_{\vec{r}_{j_3}, s} \cdot \tilde{s}_{\vec{r}_{j_4}, s}) \\ &+ (\tilde{s}_{\vec{r}_{j_1}, s} \cdot \tilde{s}_{\vec{r}_{j_4}, s})(\tilde{s}_{\vec{r}_{j_2}, s} \cdot \tilde{s}_{\vec{r}_{j_3}, s}) \\ &- (\tilde{s}_{\vec{r}_{j_1}, s} \cdot \tilde{s}_{\vec{r}_{j_3}, s})(\tilde{s}_{\vec{r}_{j_2}, s} \cdot \tilde{s}_{\vec{r}_{j_4}, s})],\end{aligned}\quad (66)$$

respectively. Here the spinon operator $\tilde{s}_{\vec{r}_j, s}$ has operator Cartesian components $\tilde{s}_{\vec{r}_j, s}^x = \frac{1}{2} [\tilde{s}_{\vec{r}_j, s}^+ + \tilde{s}_{\vec{r}_j, s}^-]$, $\tilde{s}_{\vec{r}_j, s}^y = \frac{1}{2i} [\tilde{s}_{\vec{r}_j, s}^+ - \tilde{s}_{\vec{r}_j, s}^-]$, and $\tilde{s}_{\vec{r}_j, s}^z$ and refers to the spin of a rotated electron that singly occupies the site of real-space coordinate \vec{r}_j . The spinon operators $\tilde{s}_{\vec{r}_j, s}$ and $\tilde{s}_{\vec{r}_j, s}^\pm$ are those given in Eq. (54). Furthermore, in the expressions of Eqs. (65) and (66) the summation $\langle j_1 j_2 \rangle$ runs over nearest-neighboring sites and $D_{j, j'} = 1$ for the real-space coordinates \vec{r}_j and $\vec{r}_{j'}$ corresponding to nearest-neighboring sites and $D_{j, j'} = 0$ otherwise.

For very large U/t values when electron single and double occupancy become good quantum numbers and thus the rotated electrons become electrons the spinon operators $\tilde{s}_{\vec{r}_j, s}$ become the usual spin operators $\vec{s}_{\vec{r}_j, s}$ and Eqs. (65) and (66) recover the corresponding spin-only Hamiltonian terms obtained previously by other authors.³¹ On the other hand, for the intermediate U/t values of interest for LCO the terms of the Hamiltonian t/U expansion given in of Eq. (66) in terms of spinon (rotated-electron) operators contain much more complicated higher-order terms when expressed in terms of electron creation and annihilation operators.

C. The absolute ground state of the Hubbard model on the square lattice

The antiferromagnetic long-range order of the half-filled Hubbard model on the square lattice ground state follows from a spontaneous symmetry-breaking mechanism that occurs in the thermodynamic limit $N_a \rightarrow \infty$. It involves a whole tower of low-lying energy eigenstates of the finite system. They collapse in that limit onto the ground state.

Importantly, both that ground state and the excited energy eigenstates that collapse onto it as $N_a \rightarrow \infty$ belong to the VDU subspace. One may investigate which energy eigenstates couple to the exact finite $N_a \gg 1$ and $n = 1$ and $m = 0$ ground state $|GS\rangle$ via the operator,

$$\hat{m}_s^l = \frac{1}{N_a} \sum_{j=1}^{N_a} (-1)^j \hat{s}_{\vec{r}_j, s}^l, \quad l = \pm, z. \quad (67)$$

We insert the complete set of energy eigenstates as follows:

$$\begin{aligned}\langle GS | (\hat{m}_s^l)^2 | GS \rangle &= \sum_{l_r, l_{\eta_s}} \langle GS | \hat{m}_s^l | \Psi_{l_r, l_{\eta_s}, u} \rangle \langle \Psi_{l_r, l_{\eta_s}, u} | \hat{m}_s^l | \Psi_{GS} \rangle \\ &= \sum_{l_r, l_{\eta_s}} |\langle GS | \hat{m}_s^l | \Psi_{l_r, l_{\eta_s}, u} \rangle|^2; \quad l = \pm, x_3.\end{aligned}\quad (68)$$

Only energy eigenstates $|\Psi_{l_r, l_{\eta_s}, u}\rangle$ with excitation momentum $\vec{k} = \vec{\pi}$ and quantum numbers $S_\eta = 0$, $2S_c = N_a = N$, $S_s = 1$, and $S_s^z = 0, \pm 1$ contribute to the sum of Eq. (68). We recall that the quantum numbers $S_\eta = 0$ and $2S_c = N_a = N$ remain unchanged and thus are the same as those of the ground state $|GS\rangle$. We denote by $|\Psi_{1T}\rangle$ the $S_s = 1$, $S_\eta = 0$, $2S_c = N_a = N$, and $\vec{k} = [\pi, \pi]$ lowest spin-triplet state whose excitation energy behaves as $1/N_a$ for finite $N_a \gg 1$. For the range $U/t > 4$ of interest for our studies the contribution from this lowest spin triplet state is by far the largest. For instance,

for the related spin- $\frac{1}{2}$ Heisenberg model on the square lattice the matrix-element square $|\langle GS|\hat{n}'_s|\Psi_{1T}\rangle|^2$ exhausts the sum in Eq. (68) by more than 98.7% (Ref. 37). A similar behavior is expected for the Hubbard model on the square lattice, at least provided that $U/t > 4$.

The special properties with respect to the lattice symmetry group of the lowest-energy eigenstates contributing to the linear Goldstone modes of the corresponding $S_s = 1$ spin-wave spectrum reveal the space-symmetry breaking of the $N_a \rightarrow \infty$ ground state. In the present case of the half-filled Hubbard model on the square lattice the translation symmetry is broken. Hence, as found here, both the $\vec{k} = [0,0]$ and $\vec{k} = [\pi,\pi]$ excitation momenta appear among the lowest-energy eigenstates contributing to the linear Goldstone modes of the $S_s = 1$ spin-wave spectrum. However, that the transitions to the lowest spin-triplet state $|\Psi_{1T}\rangle$ of momentum $\vec{k} = [\pi,\pi]$ nearly exhaust the sum in Eq. (68) is consistent with the first-moment sum rules of an isotropic antiferromagnet, such that no weight is generated by states of momentum $\vec{k} = [0,0]$.

One of the few exact theorems that apply to the half-filled Hubbard model on a bipartite lattice and thus on a square lattice is that for a finite number of lattice sites N_a its ground state is a spin-singlet state.¹⁶ The studies of Refs. 7 and 13 use an operator representation that differs from that used here only by unimportant phase factors. Such studies provide evidence that the $n = 1$ and $m = 0$ ground state is the only model's ground state that is invariant under the electron-rotated-electron unitary transformation. For $N_a \gg 1$ the results of those references reveal that its spin-singlet configurations refer to $N_a/2 = N/2$ independent spin-singlet two-spinon pairs. Most of the weight of these spin-singlet two-spinon pairs stems from spinons at nearest-neighboring sites, yet they have finite contributions as well from spinons located at larger distances.

Our spinon representation has been constructed to make such $N/2$ spin-singlet spinon pairs correspond to spin-neutral objects that obey a hard-core bosonic algebra. One can then perform an extended Jordan-Wigner transformation that maps them onto $N/2$ $s1$ fermions.¹³ (In the index $s1$ the number 1 refers to one spin-singlet spinon pair.) The corresponding $s1$ fermion momentum band is full for the $n = 1$ and $m = 0$ absolute ground state. It has a momentum area $2\pi^2$ and coincides with an antiferromagnetic RBZ whose momentum \vec{q} components obey the inequality

$$|q_x| + |q_y| \leq \pi. \quad (69)$$

As a result of its invariance under the electron-rotated-electron unitary transformation, the $n = 1$ and $m = 0$ absolute ground state is the only ground state that for $U/t > 0$ belongs to a single V tower. Hence, both for it and for its spin-triplet excited states that belong to the VDU subspace, the $s1$ boundary-line momenta \vec{q}_{Bs1} are independent of $U/4t$. Consistent with Eq. (69), their Cartesian components q_{Bs1x} and q_{Bs1y} obey the equations

$$q_{Bs1x} \pm q_{Bs1y} = \pi, \quad \text{or} \quad q_{Bs1x} \pm q_{Bs1y} = -\pi. \quad (70)$$

Hence, the $s1$ boundary line refers to the lines connecting $[\pm\pi, 0]$ and $[0, \pm\pi]$.

D. The spin excitations and the ground-state spinon d -wave pairing

Within our spinon operator representation the $S_s = 1$ spin-triplet excitations relative to the $n = 1$ and $m = 0$ absolute ground state involve creation of two holes in the $s1$ band along with a shift $\vec{\pi}/N_a$ of all discrete momentum values of the full c band. Under such an excitation one of the $N_a/2 = N/2$ spin-singlet spinon pairs is broken. This gives rise to two unbound spinons in the excited state whose three occupancy configurations generate the three spin-triplet states of spin projection $S_s^z = 0, \pm 1$. In the case of such spin-triplet excitations the occupancy configurations of the two holes arising in the $s1$ fermion momentum band may simulate the motion of the two unbound spinons relative to a background of $N/2 - 1$ spinon pairs, or vice versa.

The general spin-triplet spectrum has within the present spinon representation the form

$$\omega(\vec{k}) = -\epsilon_{s1}(\vec{q}) - \epsilon_{s1}(\vec{q}'), \quad \vec{k} = \vec{\pi} - \vec{q} - \vec{q}', \quad (71)$$

where $\vec{\pi} = \pm[\pi, \pm\pi]$, \vec{q} and \vec{q}' are the momentum values of the emerging two $s1$ fermion holes, and $\epsilon_{s1}(\vec{q})$ is the corresponding $s1$ fermion energy dispersion. Indeed, the results of Ref. 13 provide evidence that for the Hubbard model on the square lattice in the VDU subspace the $s1$ fermion momentum \vec{q} is a good quantum number, so that one can define a corresponding energy dispersion. However, in contrast to 1D this property does not hold for the more general problem of that model in its full Hilbert space.¹³

The Hubbard model on the also bipartite 1D lattice has the same extended global symmetry than on the square lattice. Hence, for it an operator representation similar to that used here may be introduced. The exact Bethe-ansatz solution then implicitly performs the summation of all Hamiltonian terms of even order whose leading-order terms are given in Eqs. (65) and (66). This leads to a $s1$ fermion band $\epsilon_{s1}(q)$ that in the $U/t \rightarrow 0$ limit equals the occupied part of the electron noninteracting dispersion.^{38,39} The main effect of increasing the U/t value is decreasing the $s1$ fermion band $\epsilon_{s1}(q)$ energy bandwidth. It decreases from $2t$ as $U/t \rightarrow 0$ to zero for $U/t \rightarrow \infty$.

As discussed above, expression of the Hamiltonian in terms of rotated-electron operators leads for the intermediate $U/t \in (6,8)$ range to a quantum problem in terms of rotated-electron processes similar to the corresponding large- U/t quantum problem in terms of electron processes. At half filling the main effect of decreasing U/t is the increase of the energy bandwidth of an effective band associated with the spinon occupancy configurations. Such an effective band is the $s1$ energy dispersion. Consistent with and partially motivated by the exact 1D results yet accounting both for the corresponding common global symmetry and different physics, the rotated-electron studies of Refs. 7 and 13 provide evidence that for the model on the square lattice the effective $s1$ energy dispersion $\epsilon_{s1}(\vec{q})$ involves an auxiliary dispersion,

$$\epsilon_{s1}^0(\vec{q}) = -\frac{W_{s1}^0}{2}[\cos q_x + \cos q_y]. \quad (72)$$

In the $U/t \rightarrow 0$ limit such an auxiliary dispersion reaches its maximum energy bandwidth. Similarly to 1D, in that limit

it is expected to become the occupied part of the electron noninteracting dispersion. The main effect of increasing U/t is to decrease the energy bandwidth of that dispersion and thus the magnitude of the energy scale W_{s1}^0 in Eq. (72), so that for half filling it changes from $W_{s1}^0 = 4t$ as $U/t \rightarrow 0$ to $W_{s1}^0 = 0$ for $U/t \rightarrow \infty$.

However, the $n = 1$ and $m = 0$ ground state of the 1D half-filled Hubbard model has no antiferromagnetic long-range order as $N_a \rightarrow \infty$. In the presence of that order, provided that U/t is not too small so that one can ignore the amplitude fluctuations of the corresponding order parameter, the problem can be handled for the model on the square lattice by a suitable mean-field theory. Within it the occurrence of that order is described by a $s1$ energy dispersion of the general form,^{7,13}

$$\epsilon_{s1}(\vec{q}) = -\sqrt{|\epsilon_{s1}^0(\vec{q})|^2 + |\Delta_{s1}(\vec{q})|^2}. \quad (73)$$

Here $\epsilon_{s1}^0(\vec{q})$ is the auxiliary dispersion given in Eq. (73) and the gap function $|\Delta_{s1}(\vec{q})|$ is to be determined from comparison with the spin-triplet spectrum obtained from the standard formalism of many-body physics by summing up an infinite number of ladder diagrams. (We note that, as explicitly shown in Ref. 5, the RPA studies of Sec. IV are equivalent to summing up an infinite number of such diagrams.)

We profit from symmetry and limit our analysis of the spin spectrum of Eq. (71) to the sector $k_x \in (0, \pi)$ and $k_y \in (0, k_x)$ of the (\vec{k}, ω) space. Surprisingly, quantitative agreement with the results obtained from summing up an infinite number of diagrams is reached provided that the $s1$ dispersion gap function refers to a d -wave $s1$ fermion spin-singlet spinon pairing,

$$|\Delta_{s1}(\vec{q})| = \frac{\mu^0}{2} \frac{|\cos q_x - \cos q_y|}{2}. \quad (74)$$

Moreover, from comparison with many-body physics results one finds that the inelastic coherent spin-wave spectrum is generated by processes where \vec{q} points in the nodal direction and \vec{q}' belongs to the boundary of the $s1$ band reduced zone. The remaining choices of \vec{q} and \vec{q}' either generate the inelastic incoherent continuum spectral weight or vanishing weight, respectively.

For this choice of the momenta of the two emerging $s1$ fermion holes one finds from the use of Eqs. (72)–(74) that the spin-wave spectrum corresponds to a surface of energy and momentum given by

$$\omega(\vec{k}) = \frac{\mu^0}{2} \left| \sin\left(\frac{k_x + k_y}{2}\right) \right| + W_{s1}^0 \left| \sin\left(\frac{k_x - k_y}{2}\right) \right|, \quad (75)$$

$$\vec{k} = \vec{\pi} - \vec{q} - \vec{q}'.$$

This is a particular case of the general spin spectrum of Eq. (71), which refers to the choices of the momenta $\vec{\pi}$, \vec{q} , and \vec{q}'

$$\vec{\pi} = [\pi, -\pi], \quad \vec{q} = \left[\frac{\pi}{2} - \frac{(k_x + k_y)}{2}, -\frac{\pi}{2} - \frac{(k_x + k_y)}{2} \right],$$

$$\vec{q}' = \left[\frac{\pi}{2} - \frac{(k_x - k_y)}{2}, -\frac{\pi}{2} + \frac{(k_x - k_y)}{2} \right], \quad (76)$$

for the subsector such that $k_x \in (0, \pi)$, $k_y \in (0, k_x)$ for $k_x \leq \pi/2$, and $k_y \in (0, \pi - k_x)$ for $k_x \geq \pi/2$. Moreover, for the subsector such that $k_y \in (0, \pi)$, $k_x \in (\pi - k_y, \pi)$ for $k_y \leq \pi/2$, and $k_x \in (k_y, \pi)$ for $k_y \geq \pi/2$, respectively, it corresponds to the following choices of the momenta $\vec{\pi}$, \vec{q} , and \vec{q}' :

$$\vec{\pi} = [\pi, \pi], \quad \vec{q} = \left[\frac{\pi}{2} - \frac{(k_x + k_y)}{2}, \frac{3\pi}{2} - \frac{(k_x + k_y)}{2} \right],$$

$$\vec{q}' = \left[\frac{\pi}{2} - \frac{(k_x - k_y)}{2}, -\frac{\pi}{2} + \frac{(k_x - k_y)}{2} \right]. \quad (77)$$

Note that the components of the $s1$ band momenta \vec{q} appearing in Eqs. (76) and (77) are such that $q_x - q_y = -\pi$ and thus belong to the half-filling $s1$ boundary line defined by Eq. (70), whereas those of the momenta \vec{q}' in the same equations obey the relation $q'_x = -q'_y$ so that point in the nodal directions.

For the values $U/t = 6.1$ and $t = 295$ meV used in Sec. IV in our study of the LCO spin spectrum one finds that $W_{s1}^0 \approx t/5.95$ and $\mu^0 \approx t/0.5216$ in the expressions of Eqs. (72), (74), and (75), so that $W_{s1}^0 \approx 49.6$ meV and $\mu^0 \approx 565.6$ meV. The spin-wave spectrum of Eq. (75) calculated for these W_{s1}^0 and μ^0 values refers to the middle surface plotted in Fig. 4. Its expressions corresponding to the high-symmetry directions in the BZ are given in Appendix B. The corresponding curves are plotted in the top panel of Fig. 2, along with those obtained from the many-body physics by summing up an infinite number of ladder diagrams and the LCO experimental points of Ref. 2. In Fig. 5 the same curves are plotted together with the LCO experimental points of Ref. 4. We emphasize that the intermediate sheet plotted in Fig. 4, which corresponds to the

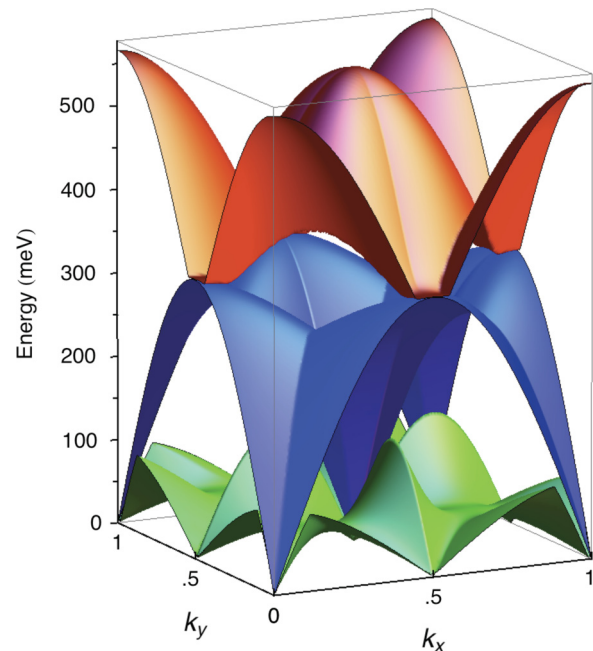


FIG. 4. (Color online) The energy-momentum space limits of the spin $S_s = 1$ excited states spectrum of Eq. (71) for $U/t = 6.1$, $t = 295$ meV, and k_x and k_y in units of 2π . States whose energy is for a given \vec{k} lower than that of the intermediate spin-wave sheet as well as those of any energy and equivalent momenta $[0, 0] = [0, 2\pi] = [2\pi, 0] = [2\pi, 2\pi]$ do not contribute to the spin spectral weight.

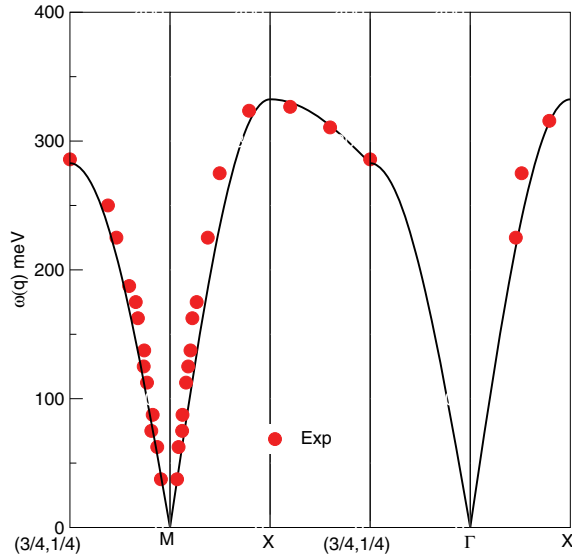


FIG. 5. (Color online) The theoretical spin spectra [Eqs. (B1)–(B9)] (solid lines) plotted in the second BZ for $U/t \approx 6.1$ and $t \approx 0.295$ eV and thus $\mu^0 = 565.6$ meV and $W_{s1}^0 = 49.6$ meV and the experimental data of Ref. 4 (circles) in meV. The momentum is given in units of 2π . From Ref. 7.

general spin-wave spectrum of Eq. (75), also fully agrees with the results of the experimental studies reported in Refs. 2 and 4.

The studies of Ref. 7 are limited to the spin-wave spectrum. Following the agreement of the spin-wave spectrum of Eq. (75) obtained from the general spin spectrum of Eq. (71) with both results from the many-body physics and LCO neutron-scattering experimental points of Refs. 2 and 4 here we consider it for all choices of the $s1$ fermion hole momenta \vec{q} and \vec{q}' . The corresponding energy-momentum space domain of the spin $S_s = 1$ excited states whose spectrum is provided in Eq. (71) is represented in Fig. 4 for $U/t = 6.1$ and $t = 295$ meV. A similar spectrum is obtained for the values $U/t = 8.0$ and $t = 335$ meV of Ref. 6.

The largest energy of the general spin spectrum of the half-filled Hubbard model on the square lattice in the VDU subspace represented in Fig. 4 is 566 meV. Hence, the whole spin spectrum of Eq. (71) represented in that figure is contained in the energy window $\omega \in (0, 2\Delta_{MH})$ of the corresponding VDU subspace. Indeed, from combination of the results of our DMRG calculations with the t magnitudes that lead to agreement with the spin-wave spectrum of LCO we have found that $2\Delta_{MH} \in (816, 1442)$ meV for $U/t \in (6, 8)$.

As mentioned above, the intermediate sheet of the general spin spectrum represented in Fig. 4 refers to the spin-wave spectrum. For each excitation momentum \vec{k} , states of energy lower than the latter spectrum do not contribute to the form-factor weight. Furthermore, and consistent with the first-moment sum rules of an isotropic antiferromagnet, no and nearly no weight is generated by states of any energy and momentum $[0, 0] = [0, 2\pi] = [2\pi, 0] = [2\pi, 2\pi]$ and near it, respectively.

Unfortunately, in its present form our spinon-operator method does not provide the detailed continuum weight intensity distribution. However, it is expected that, similarly to the Heisenberg model case,⁶ its energy-integrated intensity

follows the same trend as the spin-wave intensity. Analysis of Fig. 4 reveals that for momentum $[\pi, 0]$ there are no excited states of energy higher than the spin waves. Thus, at momentum $[\pi, 0]$, the continuum weight distribution energy-integrated intensity vanishes or is extremely small, due to $s1$ band four-hole processes. Given the expected common trend of both intensities, this is consistent with a damping of the spin-wave intensity at momentum $[\pi, 0]$, as observed in the recent high-energy inelastic neutron scattering experiments of Ref. 2 but not captured by the Fig. 2 RPA intensity. Since we find that for the half-filled Hubbard model on the square lattice the continuum weight distribution energy-integrated intensity vanishes or is extremely small at momentum $[\pi, 0]$, we predict that for it the corresponding spin-wave intensity at momentum $[\pi, 0]$ is also damped. Hence, we expect that such a behavior is absent in Fig. 2 due to the RPA used in the calculation of the spin-wave intensity. However, for all other momentum values the RPA results are expected to be a quite good estimate of the model's spin-wave intensity.

The d -wave spin-singlet spinon pairing that follows from the energy gap [Eq. (74)] emerged here from imposing quantitative agreement with the spin-wave spectrum obtained from summing up an infinite number of diagrams. We emphasize that such a type of spinon pairing is not inconsistent with the ground-state antiferromagnetic order provided that the weights of the corresponding spinon pairs fall off as a power law of the spinon distance whose negative exponent has absolute value smaller than 5. This was confirmed in Ref. 40 for spins associated with electrons yet holds as well for the present spinons, which refer to the spins of the rotated-electrons that singly occupy sites. We emphasize that such a pairing does not refer to electrons or rotated electrons. For the $n = 1$ and $m = 0$ absolute ground state it corresponds to $N/2$ spinon pairs, which describe the spin degrees of freedom of the N rotated electrons. Indeed, for that ground state all rotated electrons singly occupy sites.

VII. COMPARISON OF THE PREDICTED SPECTRAL WEIGHTS WITH THOSE IN THE LCO HIGH-ENERGY NEUTRON SCATTERING

As discussed in Sec. IV, the total spin-weight sum-rule, $\mu_B^2 2(1 - 2d)$, of Eq. (7) can in units of μ_B^2 be written as

$$W_T = 2(1 - 2d) \approx W_{SW} + W_{CO} + 4(m_{AF}^{GB})^2. \quad (78)$$

Here $W_{SW} = Z_d [2(1 - 2d) - 4(m_{AF})^2]$ is the integrated spectral weight associated with the spin-wave intensity [Eqs. (34) and (35)], $W_{CO} = (1 - Z_d) [2(1 - 2d) - 4(m_{AF})^2]$ is that of the remaining inelastic spin spectral weight associated with the continuum distribution, and $4(m_{AF}^{GB})^2$ refers to the Bragg-peak elastic part of the spin spectral weight.

In Table II we provide the results of our calculations for several integrated spin spectral weights (in units of μ_B^2). This includes the total spin spectral weight W_T and the spin-wave intensity coherent spectral weight W_{SW} . In addition, in the table we provide the estimated magnitudes of the total spin spectral weight for excitation energy $\hbar\omega \leq 450$ meV, $W_{<450} = W_{SW}/0.71 + 4(m_{AF}^{GB})^2$, and the total spin spectral weight for excitation energy $\hbar\omega > 450$ meV, $W_{>450} = [W_T - W_{<450}]$. The magnitude of the spin spectral weight for excitation

TABLE II. Several spectral weights in units of μ_B^2 as defined in the text for several U/t values and some results from Refs. 6 and 21.

U/t	6.1	6.5	8.0	10.0
W_T	1.643	1.671	1.762 [1.778 (Ref. 6)]	1.848 [1.846 (Ref. 6)]
W_{SW}	0.808	0.799	0.761	0.714
$W_{<450}$	1.571	1.593	1.663	1.730
$W_{>450}$	0.072	0.078	0.099	0.118

energy $\hbar\omega \leq 450$ meV, $W_{<450}$, is derived by combining our theoretical expressions with the observations of Ref. 2 that for the energy range up to about 450 meV, 71% and 29% of the weight corresponding to the inelastic response comes from the coherent spin-wave weight and incoherent continuum weight, respectively.

Our prediction for the magnitude of the spin spectral weight for excitation energy $\hbar\omega \leq 450$ meV, $W_{<450}$, varies between $1.6 \mu_B^2$ for $U/t \approx 6.1$ and $1.7 \mu_B^2$ for $U/t \approx 8.0$, in agreement with the experimental value $1.9 \pm 0.3 \mu_B^2$ reported in Ref. 2.

From our above analysis, the amount of spin spectral weight for excitation energy $\hbar\omega > 450$ meV is small, $W_{>450} \approx 0.1 \mu_B^2$. By combining our spectral-weight results with the boundaries of the spin-triplet spectrum plotted in Fig. 4, such a small spin spectral weight is expected to extend to about 566 meV, mostly at and around the momentum $[\pi, \pi]$.

VIII. CONCLUDING REMARKS

In this paper we have studied by means of the half-filled Hubbard model on the square lattice several open issues raised by the recent LCO neutron scattering data reported in Ref. 2. Our studies combined standard methods such as RPA techniques involving a broken-symmetry ground state with DMRG calculations on Hubbard cylinders and a spinon representation suitable to the LCO intermediate interaction range $U/t \in (6, 8)$. The latter emerges from a rotated-electron operator representation that has been constructed to ensure that rotated-electron single and double occupancy are good quantum numbers for $U/t > 0$. This assures that our spinons are well defined for the LCO intermediate U/t range. Indeed, these spinons are the spins of the rotated electrons that singly occupy sites. In the large- U/t limit the rotated-electrons become electrons, so that one recovers the usual picture.

Within this operator formulation, the Hubbard model in the VDU subspace considered here can be mapped onto a spin-only problem for the U/t range of interest for our studies. The spin excitations preserve the electron number. At fixed electron number the VDU subspace is the only one within a finite excitation-energy window, $\omega \in (0, 2\Delta_{MH})$. Here $2\Delta_{MH}$ is the Mott-Hubbard gap, whose U/t dependence we have calculated by DMRG. We have found that $2\Delta_{MH} \in (816, 1442)$ meV for $U/t \in (6, 8)$. Correspondingly, the largest energy of the general spin spectrum of the half-filled Hubbard model on the square lattice in the VDU subspace represented in Fig. 4 is 566 meV, so that it is fully contained in this energy window.

The coherent part of the spin spectrum, which corresponds to the spin-wave spectrum, was complementarily studied by a RPA analysis involving a broken symmetry ground state

and the spinon operator representation. The former method was also used to calculate the spin-wave intensity momentum distribution. Quantitative agreement with both the spin-wave spectrum obtained by summing up an infinite number of ladder diagrams and that observed in LCO neutron scattering experimental studies is reached by the spinon method provided that the initial $n = 1$ and $m = 0$ ground state has d -wave spinon pairing. For that ground state such a pairing refers only to the rotated-electron spin degrees of freedom. Whether upon hole doping such a preformed d -wave spinon pairing could lead to rotated-electron d -wave pairing or even related electron d -wave pairing is an issue that deserves further investigations.

Following the good quantitative agreement with the spin-wave spectrum, the spinon representation was used to derive the full $S_z = 1$ spin-triplet spectrum represented in Fig. 4 for the U and t values suitable for LCO. From analysis of that figure we have found that for the momentum $[\pi, 0]$ there are no excited states of energy higher than the spin waves. Thus, at momentum $[\pi, 0]$, the continuum weight distribution energy-integrated intensity vanishes or is extremely small. Such an intensity is expected to follow the same trend as that of the spin waves. Hence, this behavior is consistent with a corresponding damping of the spin-wave intensity at $[\pi, 0]$ observed in the recent high-energy inelastic neutron-scattering experiments of Ref. 2.

On the other hand, a resonant-inelastic x-ray scattering study of insulating and doped $\text{La}_{2-x}\text{Sr}_x\text{CuO}_4$ found a mode at 500 meV, at a momentum transfer $[\pi, 0]$.⁴¹ This 500-meV mode is observed only when the incident x-ray polarization is normal to the CuO planes. It could be a d-d crystal-field excitation,^{42,43} rather than a spin excitation. In case it is a spin excitation, one possible explanation given in Ref. 41 is that it involves two spin-flip processes, created on adjacent copper-oxide planes. Since our present study relies on the Hubbard model on a single square-lattice plane, that mechanism would be beyond our theoretical approach.

We recall that for each excitation momentum \vec{k} , states in the (\vec{k}, ω) domain of Fig. 4 whose energy is lower than that of the spin-wave spectrum intermediate sheet generate no spectral weight and thus do not contribute to the spin dynamical structure factor. Furthermore, consistent with the first-moment sum rules of an isotropic antiferromagnet, no and nearly no weight is generated by states of any energy and momentum $[0, 0] = [0, 2\pi] = [2\pi, 0] = [2\pi, 2\pi]$ and near it, respectively. That together with the small amount of spin spectral weight reported in Table II for energies between 450 and 566 meV indicates that in that energy window there is nearly no spin spectral weight near the momentum $[0, 0] = [0, 2\pi] = [2\pi, 0] = [2\pi, 2\pi]$ (see Fig. 4).

In addition to the Mott-Hubbard gap magnitude dependence on U/t , DMRG calculations were performed to derive the U/t dependence of the ground-state electron single occupancy expectation value $(1 - d)$. That quantity plays an important role in our study in that it controls several spin-weight sum rules. Our prediction for the amount of total spin spectral weight in the energy range $\omega \in (0, 450)$ meV quantitatively agrees with that observed in the recent high-energy inelastic neutron scattering studies of Ref. 2, which were limited to that energy window.

Moreover, as reported in Table II we predict that there is a small amount of extra weight $\approx 0.1 \mu_B^2$ above 450 meV, which extends to about 566 meV. Since at and near the momentum $[0,0] = [0,2\pi] = [2\pi,0] = [2\pi,2\pi]$ there is nearly no spin spectral weight, analysis of Fig. 4 reveals that for energies between 450 and 566 meV the small amount of extra spin spectral weight is located at and around the momentum $[\pi,\pi]$. Thus, we suggest that future LCO neutron scattering experiments scan the energies between 450 and 566 meV and momenta around $[\pi,\pi]$.

ACKNOWLEDGMENTS

We thank the authors of Ref. 2 for providing their experimental data and A. Muramatsu for discussions. J.M.P.C. thanks the hospitality of the University of Stuttgart and the support of the Portuguese FCT under Grant No. SFRH/BSAB/1177/2011, German Transregional Collaborative Research Center SFB/TRR21, and Max Planck Institute for Solid State Research. S.R.W. acknowledges the support of the NSF under Grant No. DMR 090-7500.

APPENDIX A: USEFUL OPERATORS ALGEBRA

Here we justify why the six generators of the global η spin and spin SU(2) symmetries commute with the electron-rotated-electron unitary operator. Moreover, we address the problem of the c fermion operator, spinon operator, and η -spinon operator algebras.

To achieve our first goal, it is useful to express the kinetic-energy operator \hat{T} given in Eq. (1) as $\hat{T} = \hat{T}_0 + \hat{T}_{+1} + \hat{T}_{-1}$. Here,

$$\begin{aligned} \hat{T}_\gamma &= - \sum_{(j,j')} \hat{T}_{\gamma,j,j'}, \quad \gamma = 0, \pm 1, \\ \hat{T}_{0;j,j'} &= \sum_{\sigma} [\hat{n}_{\vec{r}_j,-\sigma} c_{\vec{r}_j,\sigma}^\dagger c_{\vec{r}_{j'},\sigma} \hat{n}_{\vec{r}_{j'},-\sigma} \\ &\quad + (1 - \hat{n}_{\vec{r}_j,-\sigma}) c_{\vec{r}_j,\sigma}^\dagger c_{\vec{r}_{j'},\sigma} (1 - \hat{n}_{\vec{r}_{j'},-\sigma}) + \text{c.c.}], \\ \hat{T}_{+1;j,j'} &= \sum_{\sigma} [\hat{n}_{\vec{r}_j,-\sigma} c_{\vec{r}_j,\sigma}^\dagger c_{\vec{r}_{j'},\sigma} (1 - \hat{n}_{\vec{r}_{j'},-\sigma}) \\ &\quad + \hat{n}_{\vec{r}_{j'},-\sigma} c_{\vec{r}_{j'},\sigma}^\dagger c_{\vec{r}_j,\sigma} (1 - \hat{n}_{\vec{r}_j,-\sigma})], \\ \hat{T}_{-1;j,j'} &= \sum_{\sigma} [(1 - \hat{n}_{\vec{r}_j,-\sigma}) c_{\vec{r}_j,\sigma}^\dagger c_{\vec{r}_{j'},\sigma} \hat{n}_{\vec{r}_{j'},-\sigma} \\ &\quad + (1 - \hat{n}_{\vec{r}_{j'},-\sigma}) c_{\vec{r}_{j'},\sigma}^\dagger c_{\vec{r}_j,\sigma} \hat{n}_{\vec{r}_j,-\sigma}]. \end{aligned} \quad (\text{A1})$$

While the operator \hat{T}_0 does not change electron double occupancy, the operators \hat{T}_{+1} and \hat{T}_{-1} change it by +1 and -1, respectively.

For $U/t > 0$ the operator \hat{S} in the expression $\hat{V} = e^{-\hat{S}}$ given in Eq. (43) can be expanded in a series of t/U ,

$$\hat{S} = -\frac{t}{U} [\hat{T}_{+1} - \hat{T}_{-1}] + \mathcal{O}(t^2/U^2). \quad (\text{A2})$$

Although as discussed in Ref. 14 there are infinite choices for the operators $\hat{V} = e^{-\hat{S}}$ and \hat{S} , they share two important properties^{14,31,32}: (i) To leading order in t/U all read $-\frac{t}{U} [\hat{T}_{+1} - \hat{T}_{-1}]$, as given in Eq. (A2); (ii) their operational

expressions involve only the kinetic operators \hat{T}_0 , \hat{T}_{+1} , and \hat{T}_{-1} of Eq. (A1). Such properties apply to the specific electron-rotated-electron unitary operator \hat{V} uniquely defined in this paper.

The rotated kinetic operators \tilde{T}_0 , \tilde{T}_{+1} , and \tilde{T}_{-1} such that $\tilde{T}_\gamma = \hat{V}^\dagger \hat{T}_\gamma \hat{V}$ for $\gamma = 0, \pm 1$ are given by

$$\begin{aligned} \tilde{T}_\gamma &= - \sum_{(j,j')} \tilde{T}_{\gamma,j,j'}, \quad \gamma = 0, \pm 1, \\ \tilde{T}_{0;j,j'} &= \sum_{\sigma} [\tilde{n}_{\vec{r}_j,-\sigma} \tilde{c}_{\vec{r}_j,\sigma}^\dagger \tilde{c}_{\vec{r}_{j'},\sigma} \tilde{n}_{\vec{r}_{j'},-\sigma} \\ &\quad + (1 - \tilde{n}_{\vec{r}_j,-\sigma}) \tilde{c}_{\vec{r}_j,\sigma}^\dagger \tilde{c}_{\vec{r}_{j'},\sigma} (1 - \tilde{n}_{\vec{r}_{j'},-\sigma}) + \text{c.c.}], \\ \tilde{T}_{+1;j,j'} &= \sum_{\sigma} [\tilde{n}_{\vec{r}_j,-\sigma} \tilde{c}_{\vec{r}_j,\sigma}^\dagger \tilde{c}_{\vec{r}_{j'},\sigma} (1 - \tilde{n}_{\vec{r}_{j'},-\sigma}) \\ &\quad + \tilde{n}_{\vec{r}_{j'},-\sigma} \tilde{c}_{\vec{r}_{j'},\sigma}^\dagger \tilde{c}_{\vec{r}_j,\sigma} (1 - \tilde{n}_{\vec{r}_j,-\sigma})], \\ \tilde{T}_{-1;j,j'} &= \sum_{\sigma} [(1 - \tilde{n}_{\vec{r}_j,-\sigma}) \tilde{c}_{\vec{r}_j,\sigma}^\dagger \tilde{c}_{\vec{r}_{j'},\sigma} \tilde{n}_{\vec{r}_{j'},-\sigma} \\ &\quad + (1 - \tilde{n}_{\vec{r}_{j'},-\sigma}) \tilde{c}_{\vec{r}_{j'},\sigma}^\dagger \tilde{c}_{\vec{r}_j,\sigma} \tilde{n}_{\vec{r}_j,-\sigma}]. \end{aligned} \quad (\text{A3})$$

To confirm that the three generators of the spin SU(2) symmetry, three generators of the η -spin SU(2) symmetry, and also the momentum operator \hat{P} commute with the electron-rotated-electron unitary operator $\hat{V} = \hat{V}$, one uses the exact result that the unitary operator \hat{V} can be solely expressed in terms of the three kinetic operators given in Eq. (A1).^{14,31} In Ref. 14 the following 21 commutators were found to vanish:

$$\begin{aligned} [\hat{P}, \hat{T}_\gamma] &= [\hat{S}_\alpha^z, \hat{T}_\gamma] = [\hat{S}_\alpha^+, \hat{T}_\gamma] = [\hat{S}_\alpha^-, \hat{T}_\gamma] = 0, \\ \alpha &= \eta, s, \quad \gamma = 0, \pm 1. \end{aligned} \quad (\text{A4})$$

Although the algebra involved in their derivation is cumbersome, it is straightforward. The vanishing of the commutators given in Eq. (A4) then implies that the momentum operator and the six generators of the η spin and spin algebras commute with the unitary operator \hat{V} ,

$$\begin{aligned} [\hat{P}, \hat{V}] &= [\hat{S}_\alpha^z, \hat{V}] = [\hat{S}_\alpha^+, \hat{V}] = [\hat{S}_\alpha^-, \hat{V}] = 0, \\ \alpha &= \eta, s, \quad l = 0, \pm 1. \end{aligned} \quad (\text{A5})$$

Hence, the above operators have the same expression in terms of electron and rotated-electron creation and annihilation operators, so that the momentum operator reads

$$\hat{P} = \sum_{\sigma=\uparrow,\downarrow} \sum_{\vec{k}} \vec{k} c_{\vec{k},\sigma}^\dagger c_{\vec{k},\sigma} = \sum_{\sigma=\uparrow,\downarrow} \sum_{\vec{k}} \vec{k} \tilde{c}_{\vec{k},\sigma}^\dagger \tilde{c}_{\vec{k},\sigma}. \quad (\text{A6})$$

Furthermore, the above-mentioned six generators are given by

$$\begin{aligned} \hat{S}_\eta^z &= \sum_{j=1}^{N_a} \hat{s}_{\vec{r}_j,\eta}^z = \sum_{j=1}^{N_a} \tilde{s}_{\vec{r}_j,\eta}^z, & \hat{S}_\eta^+ &= \sum_{j=1}^{N_a} \hat{s}_{\vec{r}_j,\eta}^+ = \sum_{j=1}^{N_a} \tilde{s}_{\vec{r}_j,\eta}^+, \\ \hat{S}_\eta^- &= \sum_{j=1}^{N_a} \hat{s}_{\vec{r}_j,\eta}^- = \sum_{j=1}^{N_a} \tilde{s}_{\vec{r}_j,\eta}^-, & \hat{S}_s^z &= \sum_{j=1}^{N_a} \hat{s}_{\vec{r}_j,s}^z = \sum_{j=1}^{N_a} \tilde{s}_{\vec{r}_j,s}^z, \\ \hat{S}_s^+ &= \sum_{j=1}^{N_a} \hat{s}_{\vec{r}_j,s}^+ = \sum_{j=1}^{N_a} \tilde{s}_{\vec{r}_j,s}^+, & \hat{S}_s^- &= \sum_{j=1}^{N_a} \hat{s}_{\vec{r}_j,s}^- = \sum_{j=1}^{N_a} \tilde{s}_{\vec{r}_j,s}^-. \end{aligned} \quad (\text{A7})$$

Those of the unrotated local operators appearing here associated with the η -spin algebra read

$$\begin{aligned}\hat{s}_{\vec{r}_j,\eta}^z &= -\frac{1}{2}[1 - \hat{n}_{\vec{r}_j,\uparrow} - \hat{n}_{\vec{r}_j,\downarrow}], & \hat{s}_{\vec{r}_j,\eta}^+ &= e^{i\vec{\pi}\cdot\vec{r}_j} c_{\vec{r}_j,\downarrow}^\dagger c_{\vec{r}_j,\uparrow}^\dagger, \\ \hat{s}_{\vec{r}_j,\eta}^- &= e^{-i\vec{\pi}\cdot\vec{r}_j} c_{\vec{r}_j,\uparrow} c_{\vec{r}_j,\downarrow}, & j &= 1, 2, \dots, N_a,\end{aligned}\quad (\text{A8})$$

whereas those associated with the spin algebra are given in Eq. (4). On the other hand, the rotated local operators appearing in the alternative expressions of Eq. (A7) are provided in Eq. (54).

The six local operators given in Eqs. (4) and (A8) together with the local operator,

$$\hat{s}_{\vec{r}_j,c} = \sum_{\sigma=\uparrow,\downarrow} \hat{n}_{\vec{r}_j,\sigma} (1 - \hat{n}_{\vec{r}_j,-\sigma}), \quad j = 1, 2, \dots, N_a, \quad (\text{A9})$$

are the seven generators of the $U \neq 0$ local gauge $SU(2) \times SU(2) \times U(1)$ symmetry of the Hubbard model on a bipartite lattice with vanishing transfer integral, $t = 0$ (Ref. 19).

Since the electron-rotated-electron transformation generated by the operator \hat{V} is unitary, the rotated-electron operators $\tilde{c}_{\vec{r}_j,\sigma}^\dagger$ and $\tilde{c}_{\vec{r}_j,\sigma}$ of Eq. (43) have the same anticommutation relations as the corresponding electron operators $c_{\vec{r}_j,\sigma}^\dagger$ and $c_{\vec{r}_j,\sigma}$, respectively. Similarly, the local c fermion operators of Eq. (50) and three local spinon operators and three local η -spinon operators of Eq. (54) have the same algebra as the corresponding unrotated spinless and η -spinless fermion operators of Eq. (49) and and three local spin operators of Eq. (4) and three local η -spin operators of Eq. (A8), respectively. The former operators play a major role in the finite- U/t physics of the model. The latter operators are a limiting case of the former operators reached for $U/t \gg 1$. Hence, without loss of generality in the following we provide the algebra of the local c fermion operators of Eq. (50) and three ηs quasispin operators of Eq. (55). The $SU(2)$ algebra of the latter three operators fully determines those of the three local spinon operators and three local η -spinon operators of Eq. (54).

Straightforward manipulations based on Eqs. (50)–(55) lead to the following algebra for the c fermion operators:

$$\{f_{\vec{r}_j,c}^\dagger, f_{\vec{r}_j,c}\} = \delta_{j,j'}, \quad \{f_{\vec{r}_j,c}^\dagger, f_{\vec{r}_j',c}^\dagger\} = \{f_{\vec{r}_j,c}, f_{\vec{r}_j',c}\} = 0, \quad (\text{A10})$$

and the c fermion operators and the local ηs quasispin operators,

$$\begin{aligned}[f_{\vec{r}_j,c}^\dagger, \tilde{q}_{\vec{r}_j'}^l] &= [f_{\vec{r}_j,c}, \tilde{q}_{\vec{r}_j'}^l] = 0, \\ [f_{\vec{r}_j,c}^\dagger, \tilde{s}_{\vec{r}_j',\alpha}^l] &= [f_{\vec{r}_j,c}, \tilde{s}_{\vec{r}_j',\alpha}^l] = 0, \\ l &= \pm, x_3, \quad \alpha = \eta, s.\end{aligned}\quad (\text{A11})$$

The $SU(2)$ algebra obeyed by the local ηs quasispin operators $\tilde{q}_{\vec{r}_j}^l$ where $l = x_3, \pm$, such that $\tilde{q}_{\vec{r}_j}^\pm = \tilde{q}_{\vec{r}_j}^x \pm i \tilde{q}_{\vec{r}_j}^y$, and corresponding η -spinon ($\alpha = \eta$) and spinon ($\alpha = s$) operators $\tilde{s}_{\vec{r}_j,\alpha}^l$ is

$$[\tilde{q}_{\vec{r}_j}^+, \tilde{q}_{\vec{r}_j'}^-] = \delta_{j,j'} 2 \tilde{q}_{\vec{r}_j}^{x_3}; \quad [\tilde{q}_{\vec{r}_j}^\pm, \tilde{q}_{\vec{r}_j'}^{x_3}] = \mp \delta_{j,j'} \tilde{q}_{\vec{r}_j}^\pm, \quad (\text{A12})$$

and

$$\begin{aligned}[\tilde{s}_{\vec{r}_j,\alpha}^+, \tilde{s}_{\vec{r}_j',\alpha'}^-] &= \delta_{j,j'} \delta_{\alpha,\alpha'} 2 \tilde{s}_{\vec{r}_j,\alpha}^{x_3}, \\ [\tilde{s}_{\vec{r}_j,\alpha}^\pm, \tilde{s}_{\vec{r}_j',\alpha'}^{x_3}] &= \mp \delta_{j,j'} \delta_{\alpha,\alpha'} \tilde{s}_{\vec{r}_j,\alpha}^\pm, \\ \alpha, \alpha' &= \eta, s,\end{aligned}\quad (\text{A13})$$

respectively. Moreover, one has obviously that $[\tilde{q}_{\vec{r}_j}^l, \tilde{q}_{\vec{r}_j'}^l] = 0$ and $[\tilde{s}_{\vec{r}_j,\alpha}^l, \tilde{s}_{\vec{r}_j',\alpha'}^l] = 0$, where $l = 0, \pm$ and $\alpha, \alpha' = \eta, s$. While the c fermion and ηs quasispin operator algebras refer to the whole Hilbert space, those of the η -spinon and spinon operators correspond to well-defined subspaces spanned by states whose value of the number $2S_c$ of rotated-electron singly occupied sites is fixed. This ensures that the value of the corresponding η -spinon number $M_\eta = [N_a - 2S_c]$ and spinon number $M_s = 2S_c$ is fixed as well.

The relations given in Eqs. (A10)–(A13) confirm that when acting onto the model's Hilbert space the c fermions associated with the global c hidden $U(1)$ symmetry are η -spinless and spinless fermionic objects. They are consistent as well with the spinons and η spinons being spin- $\frac{1}{2}$ and η -spin- $\frac{1}{2}$ objects, respectively, whose local operators obey the usual corresponding $SU(2)$ algebras.

APPENDIX B: SPIN-WAVE SPECTRUM IN THE HIGH-SYMMETRY DIRECTIONS

In this appendix we study the spin-wave spectrum of Eq. (75) in the BZ high-symmetry directions. These directions correspond to those measured by high-resolution inelastic neutron scattering in LCO, as plotted, for instance, in Fig. 3(A) of Ref. 4. (Our theoretical spin-wave spectrum curves are plotted along with the more recent LCO high-energy neutron scattering points of Ref. 2 in Fig. 2.)

We denote such symmetry directions by MO , ΓO , XM , ΓX , and XO . They connect the momentum-space points $M = [\pi, \pi]$, $O = [\pi/2, \pi/2]$, $\Gamma = [0, 0]$, and $X = [\pi, 0]$ of the general spin-wave spectrum provided in Eq. (75). The use of that equation reveals that the spin-wave excitation spectrum is in such symmetry directions given by

$$\begin{aligned}\omega_{\Gamma O}(\vec{k}) &= \frac{\mu^0}{2} \sin(k_i), \\ \vec{k} &= [\pi, -\pi] - \vec{q} - \vec{q}' = [k_i, k_i], \\ k_i &= k_x = k_y \in (0, \pi/2),\end{aligned}\quad (\text{B1})$$

for s 1 fermion hole momenta,

$$\begin{aligned}\vec{q} &= [\pi/2 - k_i, -\pi/2 - k_i], \quad k_i \in (0, \pi/2), \\ \vec{q}' &= [\pi/2, -\pi/2],\end{aligned}\quad (\text{B2})$$

$$\begin{aligned}\omega_{MO}(\vec{k}) &= \frac{\mu^0}{2} \sin(k_i), \quad \vec{k} = [\pi, \pi] - \vec{q} - \vec{q}' = [k_i, k_i], \\ k_i &= k_x = k_y \in (\pi/2, \pi),\end{aligned}\quad (\text{B3})$$

for s 1 fermion hole momenta,

$$\begin{aligned}\vec{q} &= [\pi/2 - k_i, 3\pi/2 - k_i], \quad k_i \in (\pi/2, \pi), \\ \vec{q}' &= [\pi/2, -\pi/2],\end{aligned}\quad (\text{B4})$$

$$\omega_{\Gamma X}(\vec{k}) = \left[\frac{\mu^0}{2} + W_{s1}^0 \right] \sin(k_x/2),$$

$$\vec{k} = [\pi, -\pi] - \vec{q} - \vec{q}' = [k_x, 0], \quad k_x \in (0, \pi), \quad (\text{B5})$$

for $s1$ fermion hole momenta,

$$\vec{q} = [\pi/2 - k_x/2, -\pi/2 - k_x/2], \quad k_x \in (0, \pi),$$

$$\vec{q}' = [\pi/2 - k_x/2, -\pi/2 + k_x/2], \quad k_x \in (0, \pi), \quad (\text{B6})$$

$$\omega_{XM}(\vec{k}) = \left[\frac{\mu^0}{2} + W_{s1}^0 \right] \cos(k_y/2),$$

$$\vec{k} = [\pi, \pi] - \vec{q} - \vec{q}' = [\pi, k_y], \quad k_y \in (0, \pi), \quad (\text{B7})$$

for $s1$ fermion hole momenta,

$$\vec{q} = [-k_y/2, \pi - k_y/2], \quad k_y \in (0, \pi),$$

$$\vec{q}' = [k_y/2, -k_y/2], \quad k_y \in (0, \pi), \quad (\text{B8})$$

and,

$$\omega_{XO}(\vec{k}) = \frac{\mu^0}{2} - W_{s1}^0 \cos(k_x) = \frac{\mu^0}{2} + W_{s1}^0 \cos(k_y),$$

$$\vec{k} = [\pi, -\pi] - \vec{q} - \vec{q}' = [\pi, \pi] - \vec{q}'' - \vec{q}'''$$

$$= [k_x, \pi - k_x], \quad k_x \in (\pi/2, \pi)$$

$$= [\pi - k_y, k_y], \quad k_y \in (0, \pi/2), \quad (\text{B9})$$

for $s1$ fermion hole momenta,

$$\vec{q} = [0, -\pi], \quad \vec{q}' = [\pi - k_x, -\pi + k_x], \quad k_x \in (\pi/2, \pi), \quad (\text{B10})$$

or

$$\vec{q}'' = [0, \pi], \quad \vec{q}''' = [k_y, -k_y], \quad k_y \in (0, \pi/2), \quad (\text{B11})$$

respectively.

The theoretical spin excitation spectra [Eqs. (B1)–(B9)] are plotted in Fig. 5 (solid line) for $U/t \approx 6.1$ and $t \approx 0.295$ eV together with the experimental results of Ref. 4 (circles) for $T = 10$ K. Such U/t and t magnitudes correspond to $\mu^0 = 565.6$ meV and $W_{s1}^0 = 49.6$ meV in the above energy spectra. The spin-spectrum expressions provided in Eqs. (B1)–(B9) refer to the first BZ. In Fig. 5 they are plotted in the second BZ, alike in Fig. 3(A) of Ref. 4. An excellent quantitative agreement is reached for the above magnitudes of the involved energy scales.

- ¹See, for example, S. R. White and D. J. Scalapino, *Phys. Rev. B* **79**, 220504(R) (2009).
- ²N. S. Headings, S. M. Hayden, R. Coldea, and T. G. Perring, *Phys. Rev. Lett.* **105**, 247001 (2010).
- ³J. R. Schrieffer, X. G. Wen, and S. C. Zhang, *Phys. Rev. B* **39**, 11663 (1989).
- ⁴R. Coldea, S. M. Hayden, G. Aeppli, T. G. Perring, C. D. Frost, T. E. Mason, S.-W. Cheong, and Z. Fisk, *Phys. Rev. Lett.* **86**, 5377 (2001).
- ⁵N. M. R. Peres and M. A. N. Araújo, *Phys. Rev. B* **65**, 132404 (2002).
- ⁶J. Lorenzana, G. Seibold, and R. Coldea, *Phys. Rev. B* **72**, 224511 (2005).
- ⁷J. M. P. Carmelo, *Nucl. Phys. B* **824**, 452 (2010); **840**, 553(E) (2010).
- ⁸J.-Y. P. Delannoy, M. J. P. Gingras, P. C. W. Holdsworth, and A.-M. S. Tremblay, *Phys. Rev. B* **79**, 235130 (2009).
- ⁹N. M. Peres and M. A. N. Araújo, *Phys. Status Solidi* **236**, 523 (2003).
- ¹⁰S. Yan, D. A. Huse, and S. R. White, *Science* **332**, 1173 (2011).
- ¹¹P. Corboz, S. R. White, G. Vidal, and M. Troyer, *Phys. Rev. B* **84**, 041108 (2011).
- ¹²S. R. White, *Phys. Rev. Lett.* **69**, 2863 (1992).
- ¹³J. M. P. Carmelo, *Ann. Phys.* **327**, 553 (2012).
- ¹⁴J. M. P. Carmelo, S. Östlund, and M. J. Sampaio, *Ann. Phys.* **325**, 1550 (2010).
- ¹⁵O. J. Heilmann and E. H. Lieb, *Ann. N.Y. Acad. Sci.* **172**, 583 (1971).
- ¹⁶E. H. Lieb, *Phys. Rev. Lett.* **62**, 1201 (1989).
- ¹⁷C. N. Yang, *Phys. Rev. Lett.* **63**, 2144 (1989).
- ¹⁸C. N. Yang and S. C. Zhang, *Mod. Phys. Lett. B* **4**, 759 (1990); S. C. Zhang, *Phys. Rev. Lett.* **65**, 120 (1990).

- ¹⁹S. Östlund and E. Mele, *Phys. Rev. B* **44**, 12413 (1991).
- ²⁰E. Manousakis, *Rev. Mod. Phys.* **63**, 1 (1991).
- ²¹D. Baeriswyl, D. Eichenberger, and M. Menteshashvili, *New J. Phys.* **11**, 075010 (2009).
- ²²W. F. Brinkman and T. M. Rice, *Phys. Rev. B* **2**, 4302 (1970).
- ²³Walter Metzner and Dieter Vollhardt, *Phys. Rev. B* **39**, 4462 (1989).
- ²⁴For a finite-temperature quantum Monte Carlo estimation of $1 - 2d$, see T. Paiva, R. T. Scalettar, C. Huscroft, and A. K. McMahan, *Phys. Rev. B* **63**, 125116 (2001).
- ²⁵J. Brinckmann and P. A. Lee, *Phys. Rev. Lett.* **82**, 2915 (1999).
- ²⁶C. M. Canali, S. M. Girvin, and Mats Wallin, *Phys. Rev. B* **45**, 10131 (1992); C. M. Canali and Mats Wallin, *ibid.* **48**, 3264 (1993).
- ²⁷S. M. Hayden and R. Coldea (private communication).
- ²⁸A. Angelucci, *Phys. Rev. B* **51**, 11580 (1995).
- ²⁹C. Lavallo, M. Arikawa, S. Capponi, F. F. Assaad, and A. Muramatsu, *Phys. Rev. Lett.* **90**, 216401 (2003).
- ³⁰S. Östlund and M. Granath, *Phys. Rev. Lett.* **96**, 066404 (2006).
- ³¹J. Stein, *J. Stat. Phys.* **88**, 487 (1997).
- ³²A. L. Chernyshev, D. Galanakis, P. Phillips, A. V. Rozhkov, and A.-M. S. Tremblay, *Phys. Rev. B* **70**, 235111 (2004).
- ³³A. H. MacDonald, S. M. Girvin, and D. Yoshioka, *Phys. Rev. B* **41**, 2565 (1990); **37**, 9753 (1988).
- ³⁴A. B. Harris and R. V. Lange, *Phys. Rev.* **157**, 295 (1967).
- ³⁵A. S. Moskvina, *Phys. Rev. B* **84**, 075116 (2011).
- ³⁶S. Ono, S. Komiya, and Y. Ando, *Phys. Rev. B* **75**, 024515 (2007).
- ³⁷P. Horsch and W. von der Linden, *Z. Phys. B* **72**, 181 (1988).
- ³⁸J. M. P. Carmelo and P. D. Sacramento, *Phys. Rev. B* **68**, 085104 (2003).
- ³⁹J. M. P. Carmelo, J. M. Román, and K. Penc, *Nucl. Phys. B* **683**, 387 (2004).
- ⁴⁰S. Liang, B. Douçot, and P. W. Anderson, *Phys. Rev. Lett.* **61**, 365 (1988).

⁴¹J. P. Hill, G. Blumberg, Young-June Kim, D. S. Ellis, S. Wakimoto, R. J. Birgeneau, Seiki Komiyama, Yoichi Ando, B. Liang, R. L. Greene, D. Casa, and T. Gog, *Phys. Rev. Lett.* **100**, 097001 (2008).

⁴²J. D. Perkins, J. M. Graybeal, M. A. Kastner, R. J. Birgeneau, J. P. Falck, and M. Greven, *Phys. Rev. Lett.* **71**, 1621 (1993).

⁴³J. P. Falck, J. D. Perkins, A. Levy, M. A. Kastner, J. M. Graybeal, and R. J. Birgeneau, *Phys. Rev. B* **49**, 6246 (1994).